The role of CHMP2B mutations in astrocytic dysfunction: implications for neurodegeneration

by

Emma Bosworth

A thesis submitted in partial fulfilment for the requirements for the degree of
MSc (by Research) at the University of Central Lancashire

November 2017

STUDENT DECLARATION FORM

![UCLan logo - University of Central Lancashire]

Type of Award   **MSc (By Research)**

School   **Pharmacy and Biomedical Science**

*Sections marked * delete as appropriate*

1.   Concurrent registration for two or more academic awards

*I declare that while registered as a candidate for the research degree, I have not been a registered candidate or enrolled student for another award of the University or other academic or professional institution

2.   Material submitted for another award

*I declare that no material contained in the thesis has been used in any other submission for an academic award and is solely my own work

3.   Collaboration

Where a candidate's research programme is part of a collaborative project, the thesis must indicate in addition clearly the candidate's individual contribution and the extent of the collaboration. Please state below:

_____

4.   Use of a Proof-reader

*No proof-reading service was used in the compilation of this thesis.

E. Bosworth (signature)

Signature of Candidate

Print name: Emma Bosworth

Abstract

The ESCRT machinery is a group of cytosolic protein complexes whose main function is to form intraluminal vesicles. CHMP2B is a protein subunit of the ESCRT III complex which, when mutated, has been seen to cause a rare familial form of frontotemporal dementia. These mutations produce aberrant endocytic and autophagic activity within cells. Astrocytes have been implicated in virtually all neuropathologies and are responsible for a variety of key functions in the brain, one of which is glutamate regulation. CHMP2B has been reported to be ubiquitously expressed however no research has specifically investigated it in astrocytes despite their emerging role in these neuropathologies including frontotemporal dementia. This project aimed to determine CHMP2B expression in astrocytes and elucidate whether the FTD associated mutation CHMP2B^{Intron5} affected basic astrocyte biology. Western blotting and immunofluorescence staining of cell lines was conducted to confirm expression of CHMP2B in astrocytes and revealed that CHMP2B is expressed in astrocytes. Following confirmation of expression transient transfection of cells was used to create an expression model of CHMP2B^{Intron5} in order to analyse the effects of this mutation on cell morphology and localisation of the glutamate transporters EAAT1 and EAAT2. Morphological analysis showed no difference in cells when comparing CHMP2BWT and CHMP2B^{Intron5} nor was any difference in glutamate transporter localisation observed. This project did not find any alterations to basic astrocyte biology when exposed to mutations in CHMP2B.

1. Introduction

Endocytosis is an integral process within all cells to ensure proper internalisation, recycling and degradation of proteins (Piper and Katzmann, 2007). Degradation of proteins is pivotal for removal of misfolded or defective proteins to make sure aberrant signalling or aggregation does not occur. Internalisation of surface receptors is also important for regulation of cellular signalling (Babst *et al.*, 2002). In neurons, endocytosis is vitally important in recycling of synaptic vesicles and neurotransmitter receptor availability at synapses. These are fundamental to ensure neurotransmission is occurring correctly as defects in this can lead to aberrant activity within the brain (Saheki and De Camilli, 2012). Endocytosis in neurons is also important for internalisation of neuronal growth factors which initiate signalling cascades that are key for a variety of functions such as axonal growth, cell survival and dendritic branching (Cosker and Segal, 2014). Furthermore due to the length of neurons signals must sometimes travel a long way so transport via endosomes helps in signalling across long distances.

1

One specialised subtype of endosome are known as multivesicular bodies (MVBs). What makes these endosomes special is that they contain intraluminal vesicles which are formed by inward budding of the endosomal membrane away from the cytoplasm (Alonso Y Adell and Teis, 2011). This mechanism is often used for endocytosis of receptors which must be degraded in order to inhibit cellular signalling. By forming an intraluminal vesicle the signal from the receptor cannot be transmitted as it is contained within the vesicle. The formation of intraluminal vesicles is a complex task which is carried out by the endosomal sorting complex required for transport (ESCRT) machinery (Stuchell-Brereton *et al.*, 2007).

1.1 ESCRTs

The ESCRT machinery comprises a group of cytosolic protein complexes which have the unique ability to bend the membrane away from the cytoplasm in order to create intraluminal vesicles as part of the MVB pathway and also are utilised for cytokinesis (Schmidt and Teis, 2012; Woodman, 2016). There are four sub-complexes which make up the ESCRT machinery; ESCRT 0, ESCRT I, ESCRT II, ESCRT III along with the ATPase Vaculolar protein sorting-associated protein 4 (VPS4) (Alonso Y Adell and Teis, 2011). Each of these complexes has a unique and sequential role in the formation of intraluminal vesicles for the sorting of proteins within the endosome (Henne *et al.*, 2011).

ESCRT 0 is responsible for initiation of the MVB pathway and also for sorting of ubiqutinated proteins in the endosome. ESCRT I and II are thought to work together to help stabilise the vesicles that are formed (Schmidt and Teis, 2012). ESCRT III is thought to also be involved in the sorting and recycling of cargo as it is able to recruit deubiqutinases to the forming vesicles and also to provide a binding site for the final component, VPS4, to bind (Babst *et al.*, 2002). VPS4 is a AAA type ATPase (ATPases associated with diverse cellular activities) which is required for the scission of the vesicles and for disassembly of the complex (Davies *et al.*, 2009). Each of the subunits of ESCRT-III contains a microtubule interacting and trafficking interacting motif (MIM) which are important for binding and forming the ESCRT-III complex and is key for interaction with VPS4 (Stuchell-Brereton *et al.*, 2007).

ESCRT-III comprises of four core subunits; CHMP2 (A and B), CHMP3, CHMP4 (A – C) and CHMP6. Along with these there are three accessory components; CHMP1 (A and B), CHMP5 and Ist1 (Schmidt and Teis, 2012). Unlike the other ESCRT complexes, ESCRT-III does not form a stable complex in the cytoplasm so only forms transiently on endosomes when needed (Babst *et al.*, 2002). Mutations altering any subunit or accessory component can significantly affect formation of ESCRT-III and subsequently hinder its function.

Mutations affecting ESCRT III have been linked to a variety of disorders including Fragile X syndrome, hereditary spastic paraplegia, amyotrophic lateral sclerosis (ALS) and frontotemporal dementia (FTD) (Hurley, 2010; Krasniak and Ahmad, 2016; Vita and Broadie, 2017). Mutations in the ESCRT-III subunit charged multivesicular body protein 2B (CHMP2B) has been implicated in a rare familial form of FTD (van der Zee *et al.*, 2008).

1.2 CHMP2B

CHMP2B is a component of the ESCRT-III complex whose role is to provide the binding site required by the ATPase VPS4 in order to catalyse the membrane scission of intraluminal vesicles and induce dissociation of the ESCRT-III complex. Previous reports have shown CHMP2B to be expressed in all neuronal populations and is most highly expressed in the olfactory bulb and cerebral cortex (Ferrari *et al.*, 2010). Aside from its role in the ESCRT-III complex, CHMP2B has been implicated in synapse formation and synaptic plasticity (Chassefeyre *et al.*, 2015). Upon depletion of CHMP2B it has been observed that in cultured neurons there is reduction in dendritic branching and synaptic potentiation (Belly *et al.*, 2010). One report showed a correlation between CHMP2B transcription levels and amount of synaptogenesis, however there is little research and not much is known about how they may be linked (Chassefeyre *et al.*, 2015).

Structurally CHMP2B comprises a coiled coil domain at the N terminus and a MIM at its C terminus (van der Zee *et al.*, 2008). Mutations of CHMP2B linked to neurodegenerative diseases (including FTD) often occur in this MIM region and result in truncations at the C terminus. Normally VPS4 binds to CHMP2B at its MIM; however mutations which affect this region inhibit VPS4 from binding which may inhibit membrane scission and dissociation of ESCRT III (Stuchell-Brereton *et al.*, 2007). Furthermore when not required as part of ESCRT III, CHMP2B exists in an auto inhibited state wherein the N and C terminus are bound together (Krasniak and Ahmad, 2016). Mutations to the C terminus result in this binding site no longer being present thus CHMP2B cannot be inhibited. It has been reported that in some cases membrane protrusions occur on the cell surface where there are mutations in CHMP2B which may be linked to its inability to auto-inhibit itself (Krasniak and Ahmad, 2016). Furthermore mutations in CHMP2B have been seen to cause abnormal autophagic and endocytic activity (Krasniak and Ahmad, 2016).

The most common FTD-associated CHMP2B mutation occurs at a splice site of intron 5 where a G to C base change results in the intron remaining rather than being spliced out resulting in two splice variants, CHMP2B[Intron5] and CHMP2B[Δ10]. CHMP2B[Intron5] lacks the final 36 amino acids which are instead replaced with a single Valine residue (Isaacs *et al.*, 2011; Clayton *et al.*,

2015). In CHMP2B$^{\Delta 10}$ the final 36 amino acids are replaced with 29 nonsense residues. Both of these variants have been reported in a single Danish family with this mutation which causes a rare form of FTD known as FTD-3 (van der Zee *et al.*, 2008).

1.3 CHMP2B in Neurodegenerative disease

Mutations in CHMP2B have been implicated in a rare form of FTD, known as FTD-3. FTD-3 is a rare autosomal dominant form of FTD which arises due to mutations on chromosome 3. FTD, the second most common form of dementia after Alzheimer's disease, comprises a group of neurodegenerative disorders which have overlapping symptoms including atrophy of the brain in the frontal and temporal lobes, behavioural changes, language problems and reduced motor functions (Goedert *et al.*, 2012). There is considered to be an overlap between FTD and ALS due to the common overlap of symptoms observed in each disease. ALS is a disease in which there is progressive degeneration of both upper and lower motor neurons (Ince *et al.*, 2011). A recent study by Vernay *et al.* (2016) using a transgenic mouse model expressing CHMP2B^{Intron5} found that there both the behavioural and histological features observed were reminiscent of both FTD and ALS. Other research has also highlighted the possibility of ALS and FTD existing on a spectrum (Ferrari *et al.*, 2011; Radford *et al.*, 2015). Furthermore mutations in CHMP2B have been linked to cases of both sporadic and familial ALS, however this has only been observed in approximately 1% of cases (Chen *et al.*, 2013).

In studies using immunohistochemistry on post-mortem human brain tissue, CHMP2B has been found to co-localise with granuovacuolar degeneration (GVD) bodies (Yamazaki *et al.*, 2010). These GVD bodies are large double membrane-bound vacuoles containing a central granule (Funk *et al.,* 2011). GVD bodies are a common feature in Alzheimer's disease with beta amyloid accumulation seen within them (Willén *et al.*, 2017). Furthermore a correlation was found between episodic memory decline and GVD body formation in AD which implicates a role of perturbed autophagy and endocytosis in AD (Yamazaki *et al.*, 2010).

Changes to neurons have been noted in cases of CHMP2B mutation which include; axonal swelling, decrease in dendritic arborizations and a decrease in the number of mushroom spines (Chassefeyre *et al.*, 2015). Alongside this it has also been found that there were decreases in long term potentiation. This indicates a further role of CHMP2B in synaptic maintenance and generation.

It has also been seen that aggregates are present within microglia as well as neurons in cases of FTD caused by mutated CHMP2B (Isaacs *et al.*, 2011). This is probably due to the microglia attempting to clear the GVBs, however it has been shown that the aggregates within microglia

are often larger than that in neurons which could imply that the microglia also express the mutant CHMP2B.

Impairments in endocytosis have been linked to a variety of other neurodegenerative diseases including AD, Huntington's disease and Parkinson's disease (Frake *et al.*, 2015). It has been reported that neurons are more susceptible to faults in endocytosis in comparison to other cells, however the reason for this is not understood (Cosker and Segal, 2014).

Research investigating the role of CHMP2B in neurons has begun to identify its importance however no research has ever investigated the role of CHMP2B in astrocytes, a key neural cell type responsible for homeostasis in the brain. It has been stated that CHMP2B is ubiquitously expressed in the brain so it would be reasonable to assume it would also be expressed in astrocyte populations, yet this has not been experimentally confirmed. Research investigating astrocytes and their role in neurodegenerative disease is still extremely limited.

1.4 Astrocytes

A neurocentric view of neurodegenerative diseases has been held for many years in which it was thought that neurons alone were solely important in neurodegeneration. However research is demonstrating that glial cells are also affected in neurodegenerative diseases. Astrocytes have been seen to have an effect on neurodegeneration and in turn can also be affected by neurodegeneration (Maragakis and Rothstein, 2006; Lobsiger and Cleveland, 2007). It has not been well studied what role astrocytes play in neurodegenerative diseases but astrocytic dysfunction has been implicated and reported in cases of AD, ALS and Parkinson's disease (Maragakis and Rothstein, 2006).

Astrocytes are vital for normal functioning within the brain; they play roles in areas such as regulating cerebral blood flow, maintenance and formation of synapses and neurotransmitter regulation (Lobsiger and Cleveland, 2007). They also play a vital role in glutamate regulation at synapses through the expression of glutamate transporters (Malarkey and Parpura, 2008). Glutamate is the principal excitatory neurotransmitter in the brain; it is a key transmitter in both neurons and glial cells (Lobsiger and Cleveland, 2007). Astrocytes in particular are able to control glutamate levels through a variety of release and uptake mechanisms (Malarkey and Parpura, 2008). Glutamate acts as a gliotransmitter and is important for astrocytic modulation of synaptic plasticity (De Pittà and Brunel, 2016). The excitatory amino acid transporter (EAAT) family of glutamate transporters are important in glutamate regulation in astrocytes (Schousboe and Waagepetersen, 2005).There are five known EAAT transporters known as EAAT 1 – 5(Fahlke *et al.*, 2016). EAAT 1 and 2 are both expressed in astrocytes and EAAT2 is responsible for the uptake of approximately 90% of glutamate into astrocytes (Ugbode *et al.*,

2017). EAAT3 and EAAT4 are both expressed primarily in neurons while EAAT 5 is expressed in the retina (Lin *et al.*, 2012).

Changes in glutamate transporters have been implicated in various neurodegenerative diseases. For example mutations to glutamate transporters have been implicated in Alzheimer's disease (Jacob *et al.*, 2007; Cassano *et al.*, 2012; Han *et al.*, 2016). These mutations have been seen to produce accumulation of glutamate at the synapse which leads to excitotoxicity and subsequently cell death (Lin *et al.*, 2012; Han *et al.*, 2016). In Alzheimer's disease it has been reported that there is a decrease in glutamate transporter function and reduced EAAT2 expression in the brain, however it is unknown what causes this (Lin *et al.*, 2012).

It has also been reported that there is a loss of synapses in the frontal and temporal lobes in cases of FTD (Clare *et al.*, 2010). Since it is known that astrocytes play an important role in synapse regulation and that one of their main functions is glutamate handling it could be proposed that impairment to glutamate handling may play a role in this synapse loss observed. There has been very little research conducted looking at the role of the glutamate transporters in FTD so it is unknown what role they may play here. Hence more research is needed investigating these transporters in FTD.

Astrocytes are stellate shaped cells but are highly heterogeneous in their morphology and function which is a reflection of their subtype and localisation within the brain (Oberheim, Goldman and Nedergaard, 2012; Pekny and Pekna, 2016). The shape of astrocytes is vital for their particular functions in the many different roles they undertake. Astrocytes are able to change their shape and size following central nervous system damage in a process known as reactive gliosis (Olabarria *et al.*, 2010; Pekny and Pekna, 2016). Reactive gliosis aims to protect the cells of the brain from further damage through isolation of the damaged areas, reconstruction of the blood-brain barrier and remodelling of neuronal circuits (Olabarria *et al.*, 2010; Burda and Sofroniew, 2014).

1.5 Astrocytes in Neurodegenerative diseases

There have been a multitude of theories developed as to how astrocytes are affected in neurodegenerative diseases and what role they play there. These include alterations in calcium signalling, impaired glutamate transport and altered glial fibrillary acidic protein expression (Maragakis and Rothstein, 2006).

Previously it was thought that cell populations were independently vulnerable to toxicity and could not affect one another. However recent research has been challenging this idea and in

many neurodegenerative diseases non-cell autonomous effects have been implicated (Lobsiger and Cleveland, 2007; Ilieva *et al.*, 2009). For example, a study by Meyer *et al.* (2014) investigating sporadic and familial ALS found that non-cell autonomous activities by astrocytes had an effect on toxicity in motor neurons in both familial and sporadic forms of the disease. Another study wherein co-culturing of healthy neurons with glial cells expressing a mutant form of presenilin 1 found that there was inhibition of neurogenesis (Choi *et al.*, 2008).

In the case of ALS wherein there is death to motor neurons, research has shown that the motor neurons alone expressing a disease causing mutation is not enough to cause ALS (Phatnani and Maniatis, 2015). Research by Di Giorgio *et al.* (2007) found that astrocytes expressing ALS mutations directly contributed to the death of motor neurons *in vitro*. Furthermore research by Nagai *et al.* (2007) also found that these astrocytes are selectively toxic to motor neurons which provides evidence that astrocytes do play a role in ALS. Furthermore it has been seen in cases of FTD, Huntington's disease and AD that neurons which are surrounded by astrocytes harbouring mutations often develop aggregates and are more prone to cell death (Radford *et al.*, 2015).

Reactive gliosis has also been implicated in various neurodegenerative diseases including ALS and AD (Olabarria *et al.*, 2010; Verkhratsky *et al.*, 2014; Jones *et al.*, 2017). In the case of AD it has been shown that amyloid beta plaques and fragments are able to stimulate reactive gliosis (Phatnani and Maniatis, 2015). Reactive gliosis have been reported to occur in areas of neuronal loss in both ALS and FTD (Brettschneider *et al.*, 2012; Radford *et al.*, 2015). Reactive gliosis has also been implicated in FTD (Ilieva *et al.*, 2009).

Collectively, these studies indicate that astrocytes play a role in neurodegenerative diseases and therefore need to be investigated further to understand their roles and functions to offer new perspectives on such diseases and provide new targets for therapy. To date, there has been no research investigating the function of CHMP2B in astrocytes. Indeed, it remains unconfirmed whether CHMP2B is expressed in astrocytes, and if so what affect FTD-associated mutations may have on astrocytes.

This project aims to identify the effects of FTD-associated mutant forms of the protein CHMP2B on astrocytes. This will be achieved through:

1. Confirmation of CHMP2B expression in astrocytes by western blot and immunofluorescence
2. Creation of an expression model for experimentation by transient transfection of wild-type and mutant CHMP2B into HeLa and 1321N1 cell lines alongside a GFP reporter

3. Assessment of morphological changes to cells expressing mutant CHMP2B as an indicator of cellular stress
4. Investigation of changes to glutamate transporter localisation in cells expressing the CHMP2B mutation as an indicator of astrocyte function

2. Materials and Methods

2.1 Materials

2.1.1 Reagents

Unless otherwise stated all reagents used were purchased from Fisher (Loughborough, UK) and were of reagent grade or higher.

2.1.2 DNA Plasmids

All the DNA plasmids used in this project are listed in table 1. pEGFP-C1 was from Clontech. All other plasmids were a gift from Y. Goldberg (Grenoble institute of Neuroscience, Grenoble, France).

Plasmid	Gene	Protein	Short name
pEGFPC1	EGFP	Green fluorescent protein	pEGFP-C1
pcDNA3.1_CHMP2BWT	CHMP2B	Charged multivesicular body protein 2B	CHMP2BWT
pcDNA3.1_CHMP2BI5	CHMP2B	Charged multivesicular body protein 2B with intron 5 mutant	CHMP2BI5
pBI-empty		Empty Vector	pBI-empty

Table 1. List of DNA plasmids used in this project

2.1.3 Antibodies

All primary and secondary antibodies that were used for western blotting (WB) and immunofluorescence (IF) are listed in Table 2.

Antibody	Species	Origin	Dilution
Anti-CHMP2B	Rabbit	Abcam, Cambridge, UK	1:200 (IF) 1:5000 (WB)
Anti-EAAT1	Rabbit	Abcam. Cambridge, UK	1:200 (IF)
Anti-EAAT2	Rabbit	Abcam, Cambridge, UK	1:200 (IF)
Anti-beta actin	Mouse	Abcam, Cambridge, UK	1:10,000 (WB)
Goat Anti-Rabbit HRP	Goat	Abcam, Cambridge, UK	1:5000 (WB)
Rabbit Anti-Mouse	Rabbit	Abcam, Cambridge, UK	1:5000 (WB)
Alexa Fluor 555-	Goat	Invitrogen, Paisley, UK	1:200 (IF)

conjugated Anti-Rabbit			
Alexa Fluor 555- conjugated Anti-Mouse	Goat	Invitrogen, Paisley, UK	1:200 (IF)

Table 2. List of primary and secondary antibodies used in this project

2.2 Bacterial transformation and DNA Preparation

All bacterial work was carried out using aseptic technique. In order to amplify plasmid DNAs for subsequent transfections 1µg of DNA was added to 50µl of competent Stbl3 E.coli (Invitrogen) and incubated on ice for 30 minutes. Following incubation, the bacteria were heat shocked at 42°C for 45 seconds and returned to ice for a further two minutes. 250µl of SOC medium (2% Tryptone, 0.5% Yeast Extract, 10mM NaCl, 2.5mM KCl, 10mM $MgCl_2.6H_2O$, 20mM Glucose) was added and placed into a shaking incubator at 37°C for 1 hour to allow for recovery. 100µl of bacteria were then plated onto agar plates containing either ampicillin or kanamycin at a concentration of 50µg/ml and incubated at 37°C overnight. Single colonies were selected and grown overnight in 50ml of Luria-Bertani broth (Fisher). Plasmid extraction and purification was conducted using the Qiagen Hi-Speed plasmid maxi kit as per the manufactures instructions. Concentrations of DNA were determined using a NanoDrop 2000 spectrophotometer. The absorbance was measured at 260nm.

2.3 Cell Culture

The human brain astrocytoma cell line 1321N1 and the human cervical cancer cell line HeLa were cultured in Dulbecco's modified essential medium (DMEM) and Eagle's minimum essential medium (EMEM) respectively, each supplemented with 10% fetal bovine serum, 2mM L-glutamine, 1mM sodium pyruvate, 100U/ml penicillin and 100U/ml streptomycin. Both cell types were maintained at 37°C and 5% CO_2. Cell lines were passaged every 3-4 days when 80% confluency was reached. HeLa cells were used as a non-glial control as CHMP2B is known to be naturally expressed in this cell type (Atilla-Gokcumen *et al.*, 2014).

2.4 Transfections

Transfections using plasmid DNA were conducted using the Lipofectamine™ 3000 kit (Thermofisher). Cell lines were seeded onto coverslips in 12 well plates at a density of 70,000 cells and were left 24 hours to achieve approximately 60% confluency at time of transfection. Optimisation of transfections was undertaken using the pEGFPC1 plasmid as per the manufacturer's guidelines. 4 hours prior to transfection the media was changed. The cells were left in the transfection mix for 18 hours and then the media was replaced.

2.5 Fixing and Staining

Cells were fixed in 4% formaldehyde in PBS for ten minutes. This was followed by 0.1M glycine in PBS to quench any unreacted aldehydes for a further ten minutes. Membrane permeabilisation was carried out with 0.1% Triton X100 for four minutes. The primary antibodies were diluted in PBS and applied to the coverslips. These were incubated for 30 minutes and then washed three times in PBS. This was followed by incubation in the secondary antibody in the dark for 30 minutes. During incubation with the secondary antibody DAPI was also added at a concentration of 1µg/ml. The coverslips were washed again three times in PBS and then mounted onto microscope slides using ProLong Diamond anti-fade mountant (Invitrogen). Slides were left to cure for 24 hours and then were sealed using nail varnish.

2.6 Fluorescence microscopy and image analysis

The fixed cells were visualised using a Zeiss Cell Observer z-sectioning fluorescence imaging system equipped Zeiss definite focus, HXP 120 V illumination and FITC, GFP, DsRed and DAPI filter sets. Fluorescence images were acquired using × 20 PL Apo (0.8 NA), × 40 EC Plan-Neofluar (1.3 NA) oil and × 63 PL Apo (1.4 NA) oil objectives, AxioCam MRm Rev.3 CCD camera and ZEN Pro software (Carl Zeiss, Cambridge, UK).

Three coverslips and a minimum of five random fields of view were analysed for each experiment. Images were analysed using FIJI ImageJ software.

2.7 SDS PAGE and Western Blotting

Cells were lysed in RIPA lysis buffer (50mM Tris, 150mM NaCl, 0.5% sodium deoxycholate, 1% Triton X-100, 0.1% SDS and a Halt^{TM} Protease Inhibitor Single-Use Cocktail). A Pierce BCA assay kit (Thermo Scientific) was used to determine protein concentration in each lysate sample as per the manufacturer's guidelines. 10µg of each sample was mixed with equal volumes of 2x Laemmli buffer and boiled for five minutes. Samples were loaded onto a Bio-Rad Mini-PROTEAN 10% Tris-Glycine gel and run at 100V for 90 minutes in 1x Tris/Glycine/SDS running buffer (Bio-Rad, Watford, UK). The resolved proteins were transferred onto nitrocellulose at 300mA for 90 minutes in 1x Tris/Glycine transfer buffer (Bio-Rad). The blot was blocked overnight in 5% milk in tris-buffered saline and tween 20 (TBST) at 4°C. The blot was then probed in the anti-CHMP2B primary antibody for 4 hours. Following incubation in the primary antibody the blot was washed three times for five minutes each before the secondary antibody was applied and incubated for 1 hour. The blot was then washed again before ECL reagent was applied and visualisation was conducted using Bio-Rad Gel Doc XR+ system. The blot was then stripped and re-probed using anti-beta actin for use as a loading control.

2.8 Statistical analysis

All statistical analysis was conducted using IBM SPSS Statistics 24. Unless otherwise stated all data was normally distributed (as determined via Q-Q plots and Shapiro Wilks test) and had equal variances (Homogeneity of Variance test). Multiple comparisons were carried out using a One-way ANOVA followed by Tukey's *post-hoc*. A p-value of 0.05 or lower was considered significant throughout.

3. Results

3.1 Confirmation of CHMP2B in astrocytes

In order to confirm basal expression of CHMP2B in astrocytes; whole cell lysates of the glioma cell line 1321N1 (a commonly used astrocyte cell line) and primary normal human astrocytes were analysed by SDS-PAGE and western blot using an established and commercially available CHMP2B antibody. HeLa cells were used as both a non-glial control and as a positive control, as CHMP2B expression in this cell line has already been confirmed elsewhere. At a standard load of 10μg per lane, a single band was observed at approximately 25kDa for all cell types, corresponding to the size of CHMP2B which has a predicted molecular weight of 24kDa (Figure 3.1.1 A). All bands appeared to be of a similar thickness with the HeLa cells being slightly fainter. An anti-beta actin antibody was used as a loading control. The levels of actin appeared to be similar in the NHA's and 1321N1 cell line, but the band in the HeLa cells was much fainter indicating an unequal load. In order to overcome these apparent loading issues and to provide a semi-quantitative measure of relative CHMP2B levels in each cell type, densitometry was performed on the western blot using ImageJ (Figure 3.3.1 B). The relative densities were generated by normalisation of the CHMP2B bands against the beta actin band. Normal human astrocytes were seen to have the highest relative density at 2.05 which was followed by 1321N1 cells with a relative density of 0.79. HeLa cells had the lowest relative density at 0.43. It was only possible to undertake densitometry on a single blot due to issues with blot quality, hence statistical analyses could not be carried out.
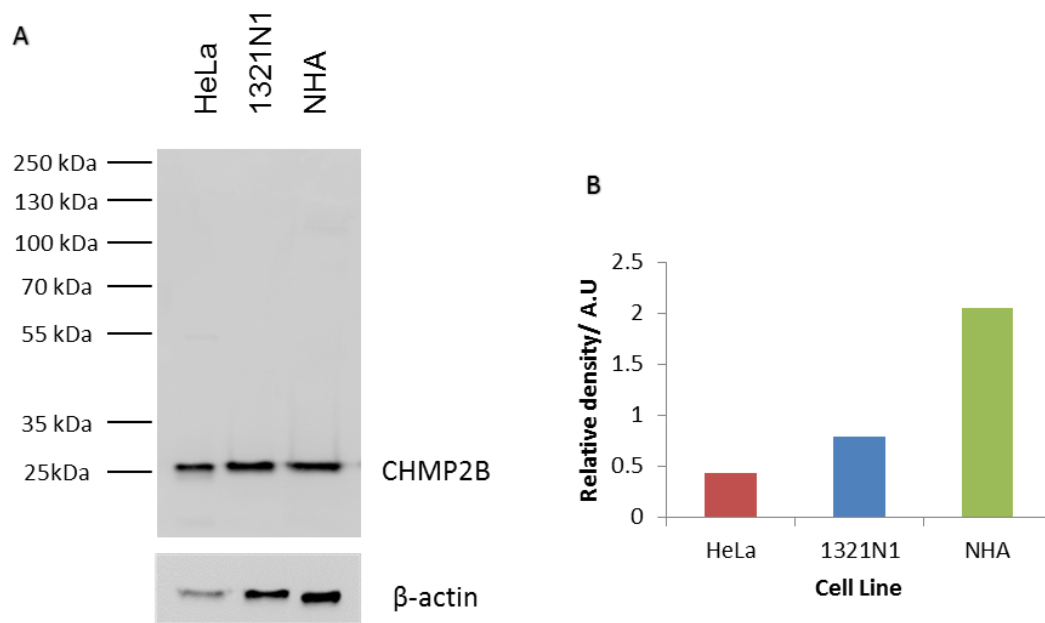
Figure 3.1.1 (A) Western blotting was used to confirm basal expression of CHMP2B in astrocytes. A single band was observed in each lane at 25kDa which corresponds with the predicted size of CHMP2B. Actin was used as a loading control and all samples were loaded at 10μg. (B) Densitometry was performed using ImageJ and the values were normalised against β-actin. NHA's were seen to have the highest relative density, followed by 1321N1 and then HeLa cells.

Further confirmation of basal CHMP2B expression in astrocytes was completed using immunocytochemistry and fluorescence microscopy. Validation of primary antibodies was undertaken, initially in HeLa cells. Unstained cells were used as negative controls and showed no signal in the dsRED channel (Figure 3.1.2 A-C). When the primary anti-CHMP2B antibody was used alone no fluorescence was observed (Figure 3.1.2 D-F). This was the same when the Alexa-Fluor 555-conjugated secondary antibody alone was used (Figure 3.1.2 G-I). When the anti-CHMP2B antibody was followed with the secondary antibody fluorescence was seen in all cells, as expected.
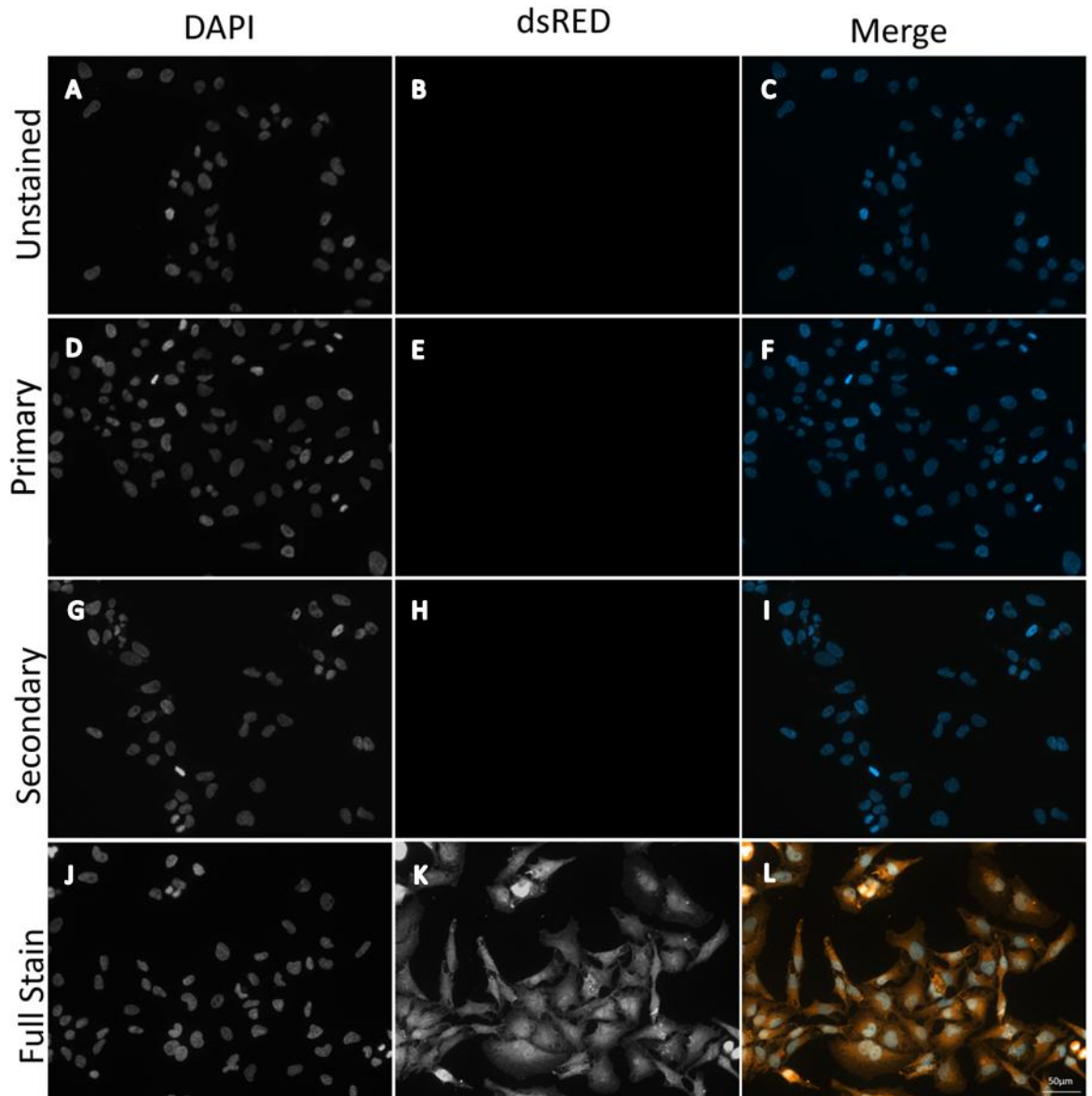
Figure 3.1.2. HeLa cells were stained for CHMP2B. Antibody controls were carried out to specificity of the antibody. Unstained cells (A-C), primary antibody only (D – F), secondary antibody only (G-I), primary and secondary antibodies (J-L). Images taken at 20x magnification. Scale bar 50µm. n=3

Antibody validation of the anti-CHMP2B antibody was then completed in 1321N1 cells to ensure the staining was similar to HeLa cells. For this unstained cells were used as controls from which to compare all other conditions to, wherein no fluorescence was seen in the dsRED channel (Figure 3.1.3 A-C). Both the cells which had been treated with the primary antibody only or the secondary antibody only were visually identical to the unstained cells in the dsRED channel as no fluorescence was seen (Figure 3.1.3 D-I). When both the primary and secondary antibodies were used in conjunction staining was observed in 1321N1 cells in the same manner as the HeLa cells. This further confirms the expression of CHMP2B in astrocytes.

15
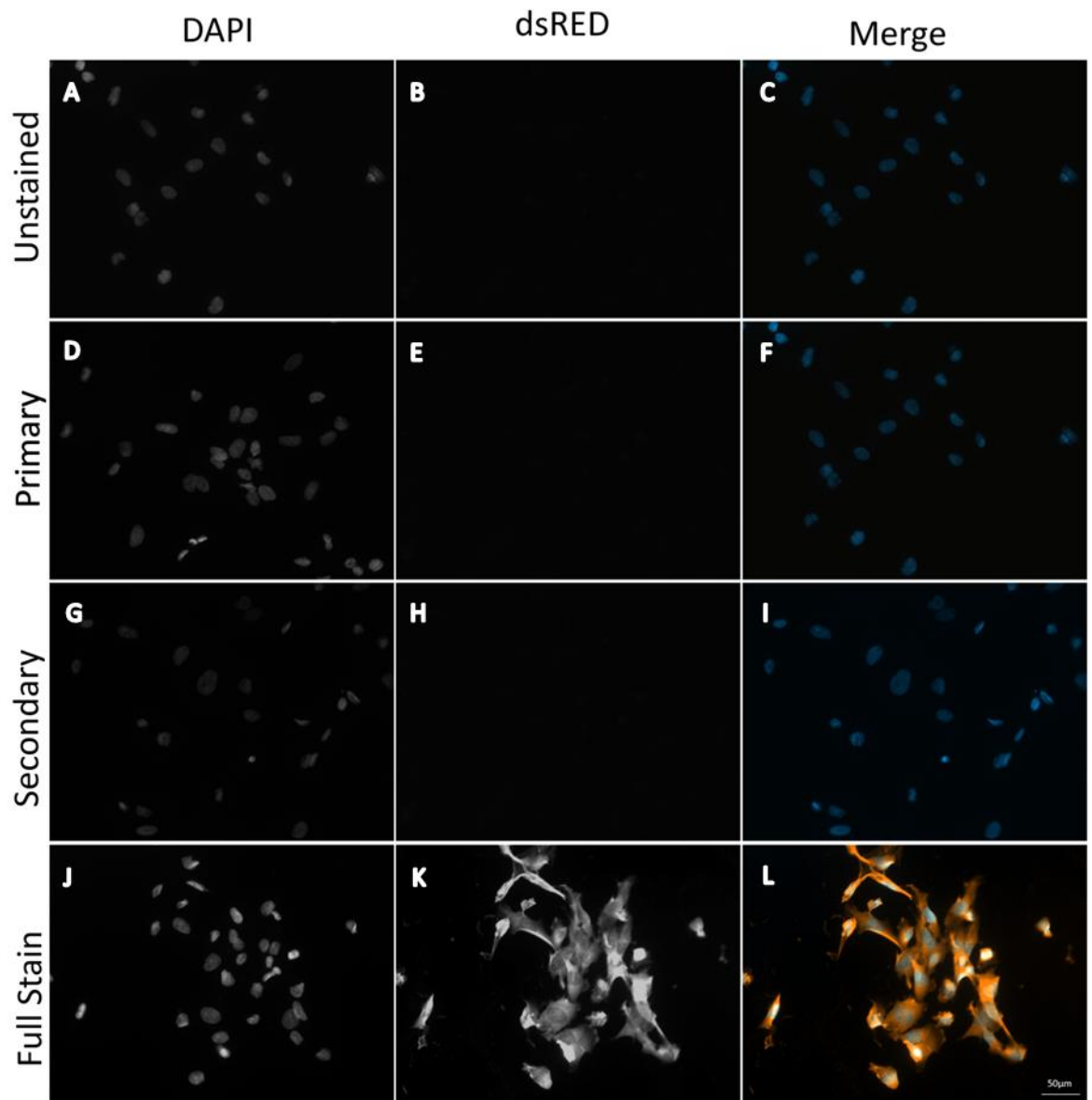
Figure 3.1.3. Staining of 1321N1 cells was carried out using anti-CHMP2B antibody to determine expression within astrocytes. Unstained cells (A-C), primary antibody only (D – F), secondary antibody only (G-I), primary and secondary antibodies (J-L). Images taken at 20x magnification. Scale bar 50μm. n=3

Mean fluroescence intesities of the cells stained for CHMP2B were measured using imageJ and compared to determine if any differences in expression levels were seen btween the two cell types. No significant difference was found between the fluroescence intensities of the two cell types. The mean pixel density for HeLa cells was 4,105,558 ± 815,404 whilst the 1321N1 cells had a mean pixel density of 3,882,177 ± 1,378,401(n=10).
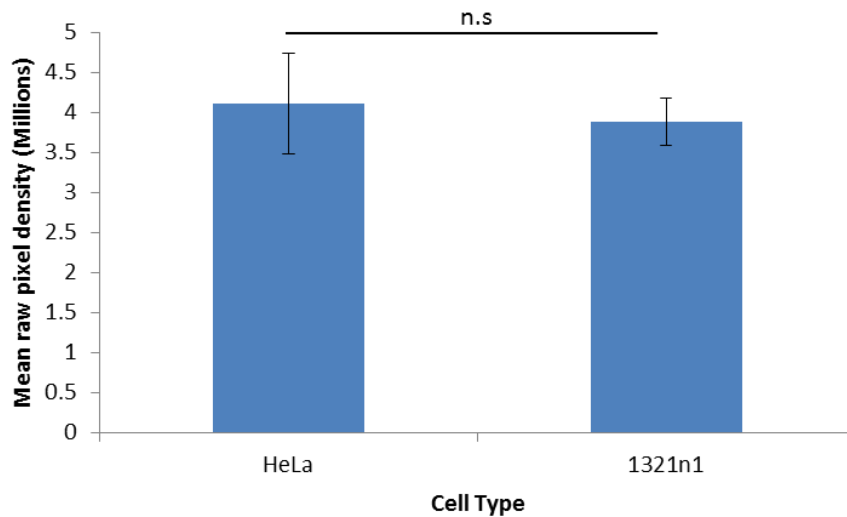
Figure 3.1.4 The fluorescence intensity of untransfected cells measured with imageJ compared between HeLa cells and 1321N1 cells. No significant difference was observed in fluorescence intensity between the cell types. n=10 fields of view. Error bars show SD.

In order to gain insight into the sub-cellular localisation pattern of CHMP2B in astrocytes, high magnification fluorescence images were taken 1321N1 cells and HeLa cells. The high magnification images showed CHMP2B expression throughout the cell in a punctate manner but absent from the nucleus in both cell types (Figure 3.1.5).
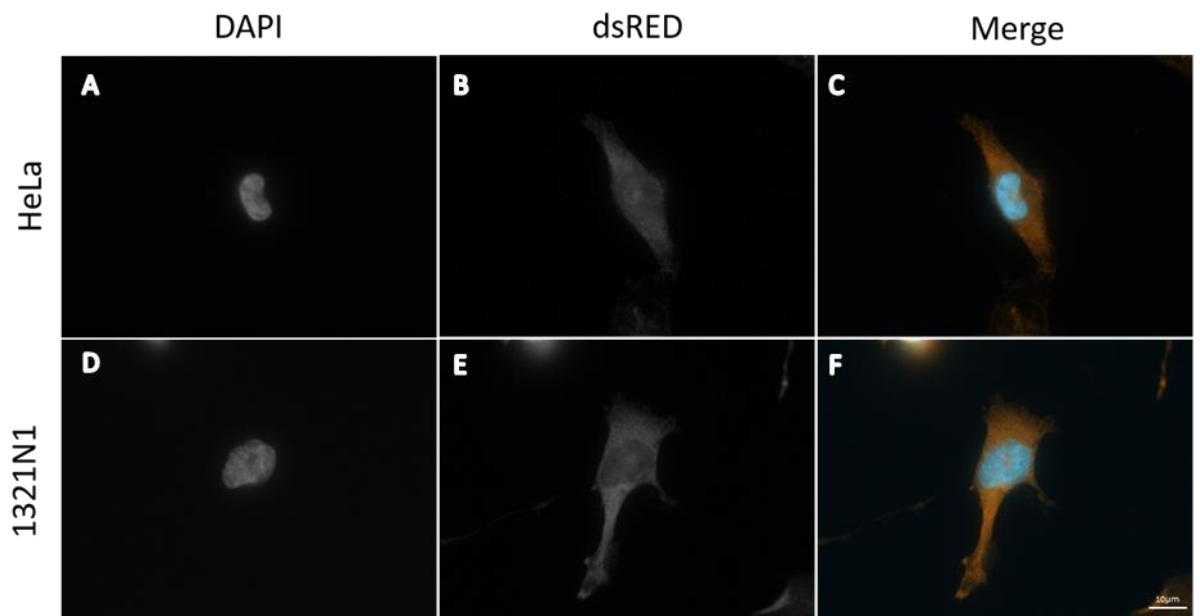
Figure 3.1.5. High magnification images of CHMP2B expression in HeLa cells and 1321N1 cells Images taken at 63x magnification. Scale bar 10μm. n=3

3.2 Creation of GFP expression model

Following confirmation of CHMP2B expression in astrocytes it was necessary to express mutant forms of the protein. An expression model was created using Lipofectamine 3000™ (referred to herein as simply Lipofectamine) reagent to allow transient transfection of DNA encoding wild-type or mutant CHMP2B to the 1321N1 astrocyte cell line and HeLa cells, as a non-astrocyte control.

To optimise the transfection protocol, different ratios of Lipofectamine reagent and DNA were trialled. pEGFP-C1 was utilised in these experiments to permit simple quantification of transfected cells by virtue of them being positive for expression of GFP. Varying ratios of Lipofectamine to DNA were trialled; 1.5µl, 2µl and 3µl of Lipofectamine reagent were used with 1µg or 2µg of DNA (Figure 3.2.1).
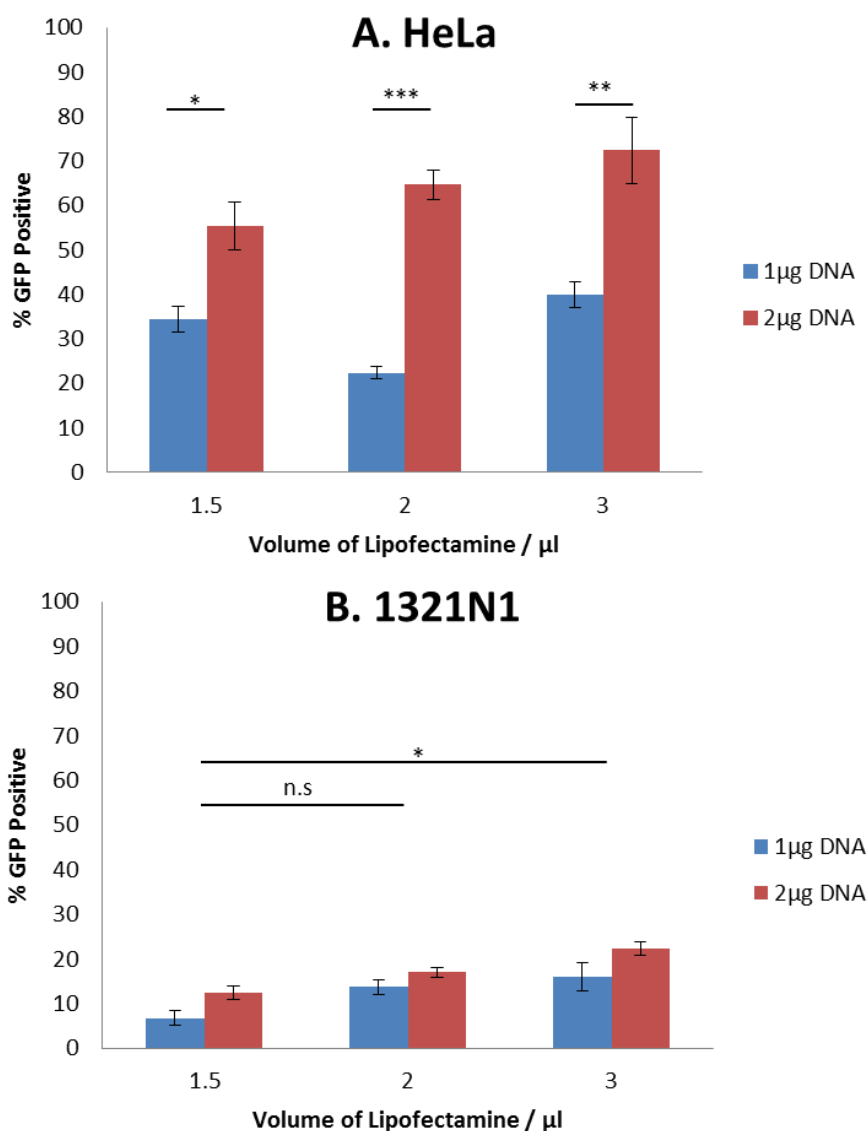
Figure 3.2.1. GFP was used to optimise the transfection protocol using differing volumes of Lipofectamine reagent and different quantities of DNA. Both 1μg and 2μg of DNA were tested; it was found that in HeLa cells (A) that 2μg of DNA significantly improved percentage of GFP positive cells across all Lipofectamine. In 1321N1 cells (B) no significant difference was observed between 1μg and 2μg DNA. However a significant difference was observed between 1.5μl and 3μl of Lipofectamine at 2μg DNA. n=3 Error bars, SEM. *p<0.05, **p<0.01, ***p<0.001.

In the case of the HeLa cells, 2μg of DNA gave a consistently higher percentage of GFP positive cells across all Lipofectamine volumes (ANOVA $F_{(5,12)}$=19.036, p<0.001; Figure 3.2.3A). Although a trend towards higher volumes of Lipofectamine yielding a greater percentage of transfected cells was seen, overall there was no significant difference in the percentage of transfected cells across the reagent volumes tested. For 1321N1 cells, there was no significant difference in transfection efficiency between 1μg and 2μg DNA across any volume of Lipofectamine; however, with 2μg DNA a volume of 3μl Lipofectamine (but not 2μl) did prove significantly more effective than 1.5μl (ANOVA $F_{(5,12)}$=7.851, p=0.002; Figure 3.2.3B). Hence, it was determined that a ratio of 3μl of Lipofectamine reagent with 2μg of DNA would be most

effective across both cell types. For the HeLa cells an average 72.3±7.5% of cells were transfected at this ratio while in the 1321N1 cells it resulted in an average efficiency of 22.3±1.5%. The ratio of 2µg DNA and 3µl Lipofectamine was therefore used for all subsequent transfections.
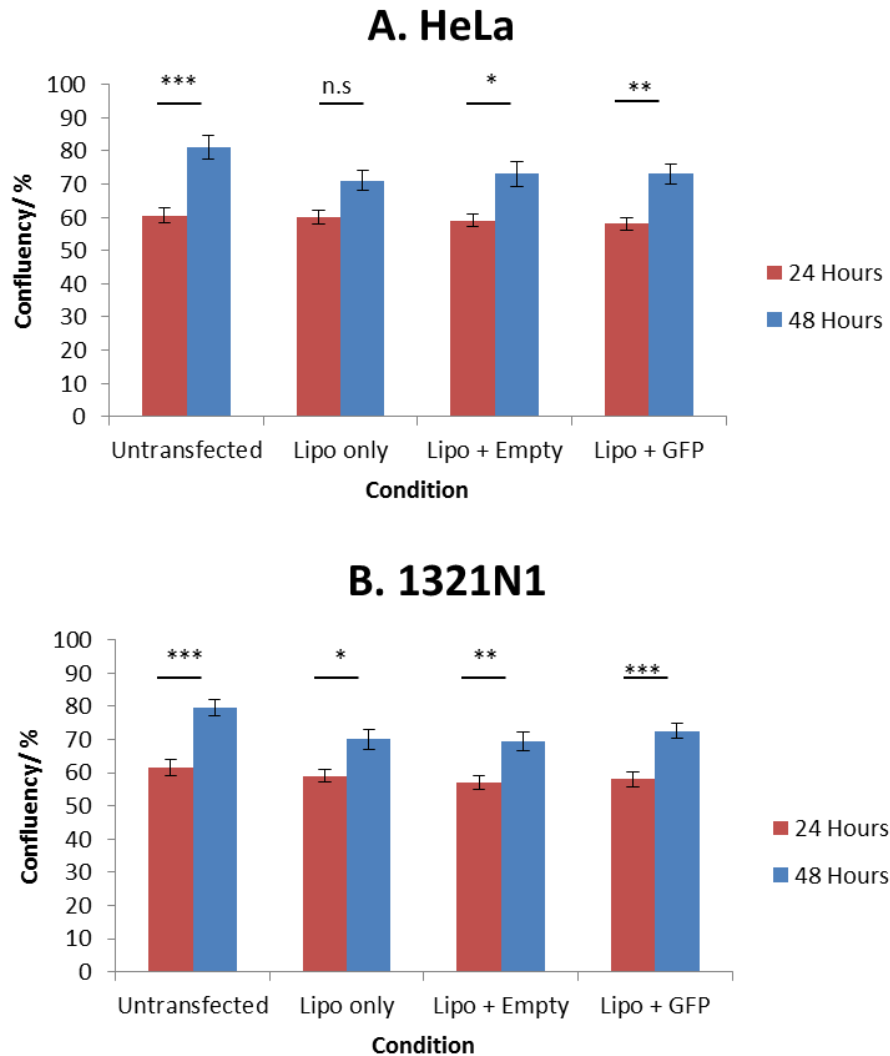
A. HeLa

B. 1321N1

Figure 3.2.2. Comparison of cell growth under different transfection conditions. Cell confluency was measures at 24 and 48 hours after seeding for untransfected cells, cells treated with Lipofectamine only, Lipofectamine pBI Empty, and Lipofectamine with pEGFP-C1 in HeLa cells (A) and 1321N1 cells (B). In both cell types there was no significant difference between the conditions at either 24 or 48 hours. n=10, error bars show SEM, *p<0.05, **p<0.01, ***p<0.001.

Once it was determined which ratio of DNA to Lipofectamine to use further, experiments were conducted to identify any effects from Lipofectamine treatment on cell growth. Both HeLa and 1321N1 cells were subjected to treatment with Lipofectamine only (to test the direct effect of this reagent on cell growth), Lipofectamine plus an empty vector (pBI-empty; to assess the effect of lipid-DNA particles on cell growth) and lipofectamine plus an expressing vector (pEGFP-C1; to address the effects of CMV-mediated overexpression of a protein on growth).

For each cell type, a control of untransfected cells was used; these cells underwent a normal medium change at the time the treatment groups were exposed to lipofectamine. Cell confluency was estimated at 24 and 48 hours post-treatment to determine if any condition impacted cell growth or survival. Cell growth changes were compared using a one-way ANOVA and Tukey's *post-hoc*. For both cell types, in all but one case, there was a significant increase in cell confluency between 24 and 48-hours post-treatment, indicating that cells continued to grow irrespective of treatment (HeLa, $F_{(7,72)}$=9.960, p<0.001; 1321N1, $F_{(7,72)}$=11.656, p<0.001; Figure 3.2.2). In the case of the Lipofectamine only-treated HeLa cells, there was an increase seen between 24 and 48 hours in all repeats, however this was shown to be not significant (p=0.099). Comparisons between treatments revealed no significant difference in confluency levels for either cell type under any treatment condition when compared to the non-transfected control. Hence, the project proceeded on the basis that Lipofectamine had no negative impact on cell growth.

In order to ensure the transfection protocol was capable of delivering the DNA plasmids and also non-toxic to the cells, pEGFP-C1 was used to allow visualisation of cells that had been successfully transfected (Figures 3.2.3 and 3.2.4). The protocol was first tested in HeLa cells due to their known ease to transfect.

Untransfected cells were used as a control from which to determine what effect Lipofectamine and plasmid DNA had on cells (Figure 3.2.3 A-C). Lipofectamine only controls showed lower numbers of cells than the untransfected cells but did not look visibly different in any way (Figure 3.2.3 D-F). When cells were transfected using an empty vector they were visually identical to the untransfected cells also (Figure 3.2.3 G-I). In all controls no fluorescence was seen unlike in the cells transfected with pEGFP-C1 which were mostly positive for GFP (Figure 3.2.3 J-L).
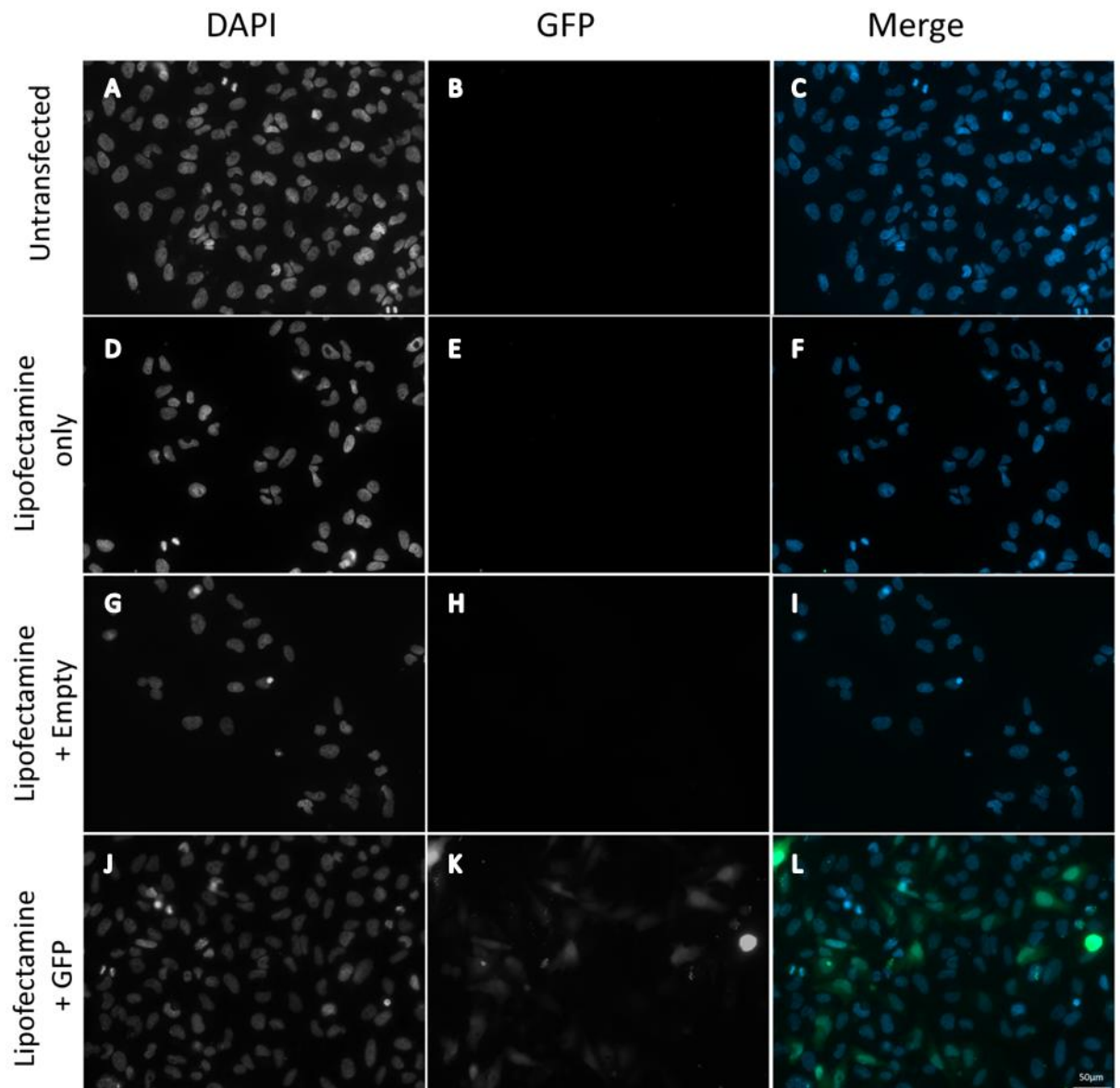
Figure 3.2.3. To determine transfection efficiency in HeLa cells GFP was used. Comparison was made between untransfected cells (A – C), cells treated with only lipofectamine (D-F), lipofectamine and an empty vector (G-I) and lipofectamine and GFP (J-L). Only the cells transfected with GFP showed fluorescence above background levels. Images were taken at 20x magnification. Scale bar 50µm. n=3

Following successful transfection in HeLa cells the same protocol was carried out in the 1321N1 cell line (Figure 3.2.4). Untransfected cells showed no fluorescence in the GFP channel and were again used as a control from which to compare all other slides to (Figure 3.2.4 A-C). Lipofectamine only slides also showed a lower number of cells which was also seen with HeLa cells but were otherwise identical to untransfected cells (Figure 3.2.4 D-F). Lipofectamine plus empty vector also showed no difference to untransfected cells (Figure 3.2.2 G-I). Finally for the Lipofectamine and GFP condition, a small proportion of cells were positive for GFP, but this was in fewer cells when compared with the HeLa cells (Figure 3.2.4 J-L).
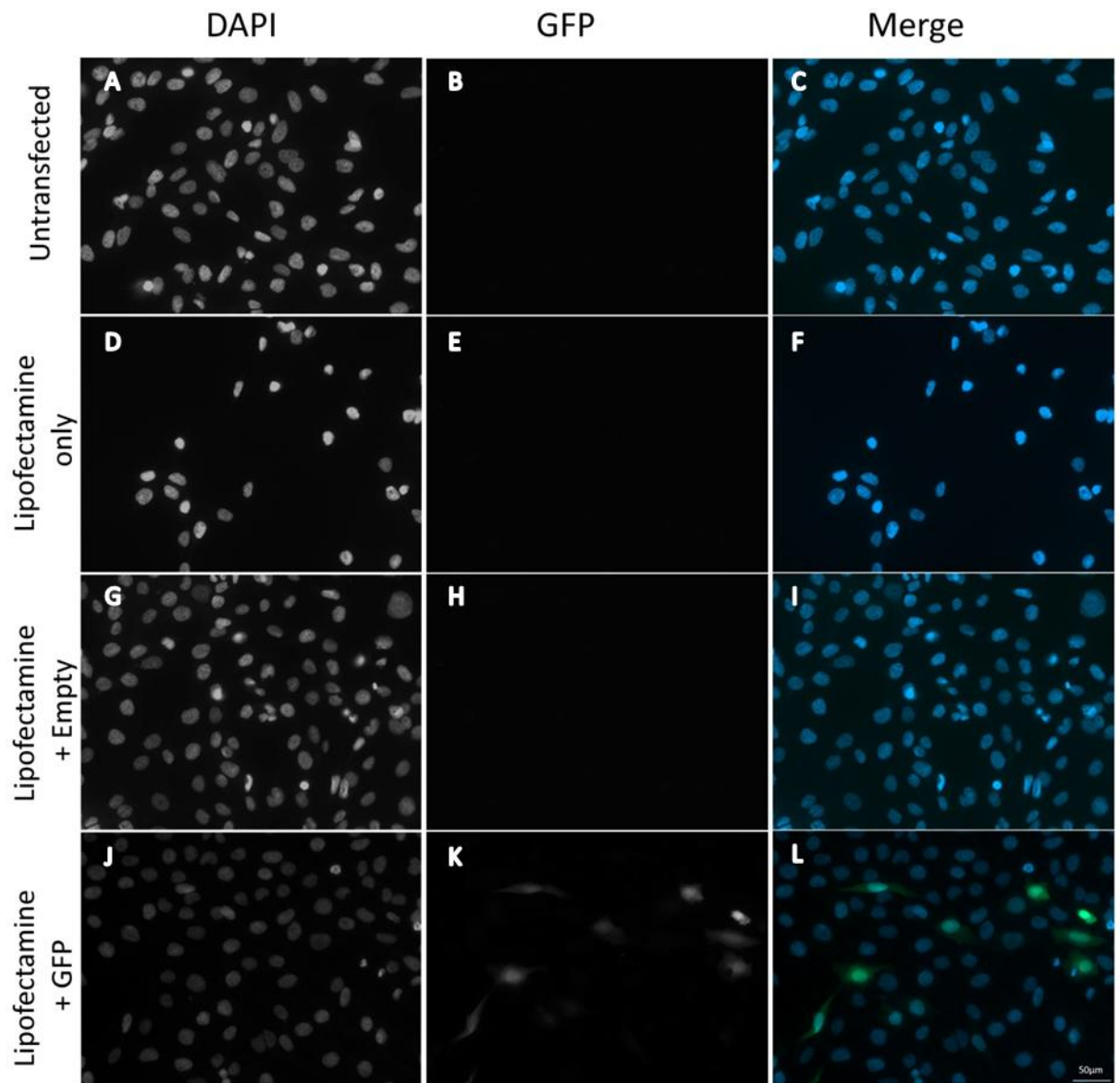
Figure 3.2.4. To determine transfection efficiency in 1321N1 cells GFP was used. Comparison was made between untransfected cells (A – C), cells treated with only lipofectamine (D-F), lipofectamine and an empty vector (G-I) and lipofectamine and GFP (J-L). Only the cells transfected with GFP showed fluorescence above background levels. Images were taken at 20x magnification. Scale bar 50μm n=3

In order to determine which cells had been transfected with the CHMP2B plasmid (which had no tag), it would later be necessary for co-transfections with pEGFP-C1 to be carried out. All lipid-based transfection reagents (including Lipofectamine) work by creating small liposomes in an aqueous solution containing plasmid DNA. Hence, the liposomes sequester the DNA from the solution within the resultant lipid-DNA complexes; thus, liposomes created in a mixed solution of different DNAs should, in theory, contain a mix of the available DNAs. This property was utilised within this project to mediate delivery of CHMP2B together with pEGFP-C1 to cells. It was necessary to optimise the co-transfections protocol; initially using pBI empty

alongside pEGFP-C1. A constant level of 2µg of DNA was utilised, either as 2µg of pEGFP-C1 alone or 1µg of pEGFP-C1 alongside 1µg pBI-empty. The same three volumes of Lipofectamine were tested as for the single transfections.

Co-transfection efficiencies were significantly lower in HeLa cells when compared to pEGFP-C1 only transfections for all volumes of Lipofectamine tested (ANOVA $F_{(5,12)}$=15.734, p<0.001; Figure 3.2.5A). Although a trend towards higher volumes of lipofectamine yielding higher transfection efficiencies with 1.5µl lipofectamine having an average efficiency of 27.33±2.52% of GFP positive cells while 3µl of lipofectamine produced an average of 40±3.0% of GFP positive cells, there was no significant difference between the volumes. For 1321N1 cells, co-transfection significantly reduced transfection efficiencies when performed with both 2µl and 3µl Lipofectamine (ANOVA $F_{(5,12)}$=21.157, p<0.001; Figure 3.2.5B). Again, a trend towards higher Lipofectamine volumes producing higher numbers of GFP positive cells was seen with 1.5µl of lipofectamine only achieving an average of 6.67±1.53% of cells GFP positive while 3µl of lipofectamine producing on average 12.33±2.52% of cells, but this was not significant at any level.
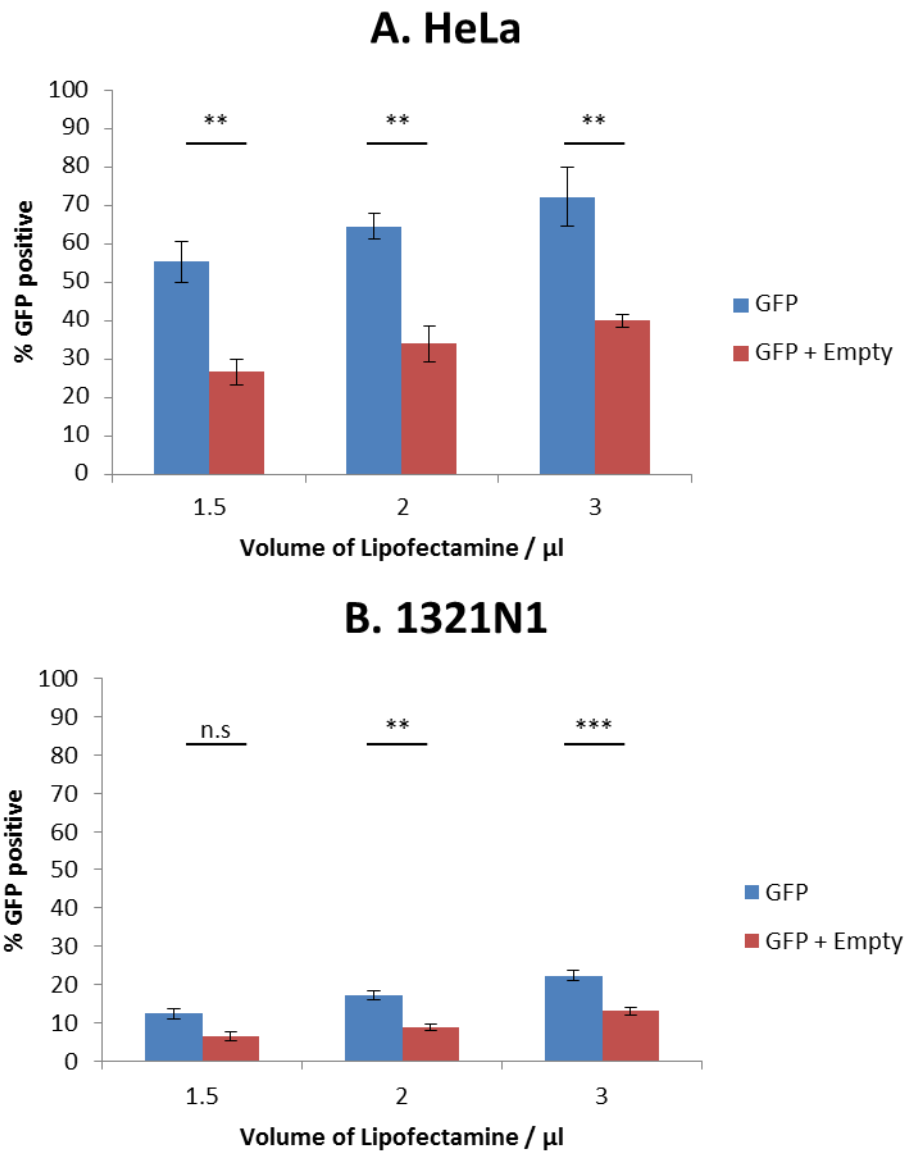
A. HeLa

B. 1321N1

Figure 3.2.5. Co-transfection efficiencies were calculated and compared to GFP-only transfections in both HeLa (A) and 1321N1 (B) cell lines. 2µg of total DNA was used (in the case of the double transfection, 1µg each of pEGFP-C1 and pBI empty). For HeLa cells (A), a significant difference was observed between single transfection and co-transfection for all volumes however no significance was seen between lipofectamine volumes for the co-transfections. In 1321N1 cells (B) significance was seen between single and co-transfections for both 2µl and 3µl lipofectamine but no significant difference was observed between lipofectamine volumes in these cells either. n=3 Error bars SEM

3.3 Expression of CHMP2B

Once the co-transfection protocol was optimised using pEGFP-C1 and pBI Empty, the expression model was created using the CHMP2B plasmids and pEGFP-C1 co-transfection in cell lines to investigate the effects that the mutant variant, CHMP2BI5, has on cellular morphology and localisation of CHMP2B.

HeLa cells were transfected first due to being easier to transfect than 1321N1 cells. Untransfected cells were used as a baseline from which to compare all other conditions to which were stained with anti-CHMP2B antibody and as expected showed no fluorescence in the GFP channel (Figure 3.3.1 A-D). Controls were set up to ensure any changes observed in the cells were due to the change in CHMP2B DNA and not any other factor. Lipofectamine only controls contained fewer cells than other conditions but showed no visible differences in terms of cellular morphology or CHMP2B staining intensity when compared to the untransfected cells otherwise (Figure 3.3.1 E-H). Lipofectamine plus pBI empty controls also showed no visible differences to the untransfected cells (Figure 3.3.1 I-L). Lipofectamine plus pEGFP-C1 showed approximately 70% of cells positive for GFP in HeLa cells (Figure 3.3.1 M-P). The Lipofectamine plus CHMP2BWT condition also showed no visible difference when compared to the untransfected control. As the cells already expressed a high basal level of CHMP2B, no visual differences were seen and thus it was impossible to tell if the CHMP2B had been successfully transfected (Figure 3.3.1 Q-T). The final condition was Lipofectamine plus both pEGFP-C1 and CHMP2BWT and approximately 40% of cells were positive for GFP (Figure 3.3.1 U-X).
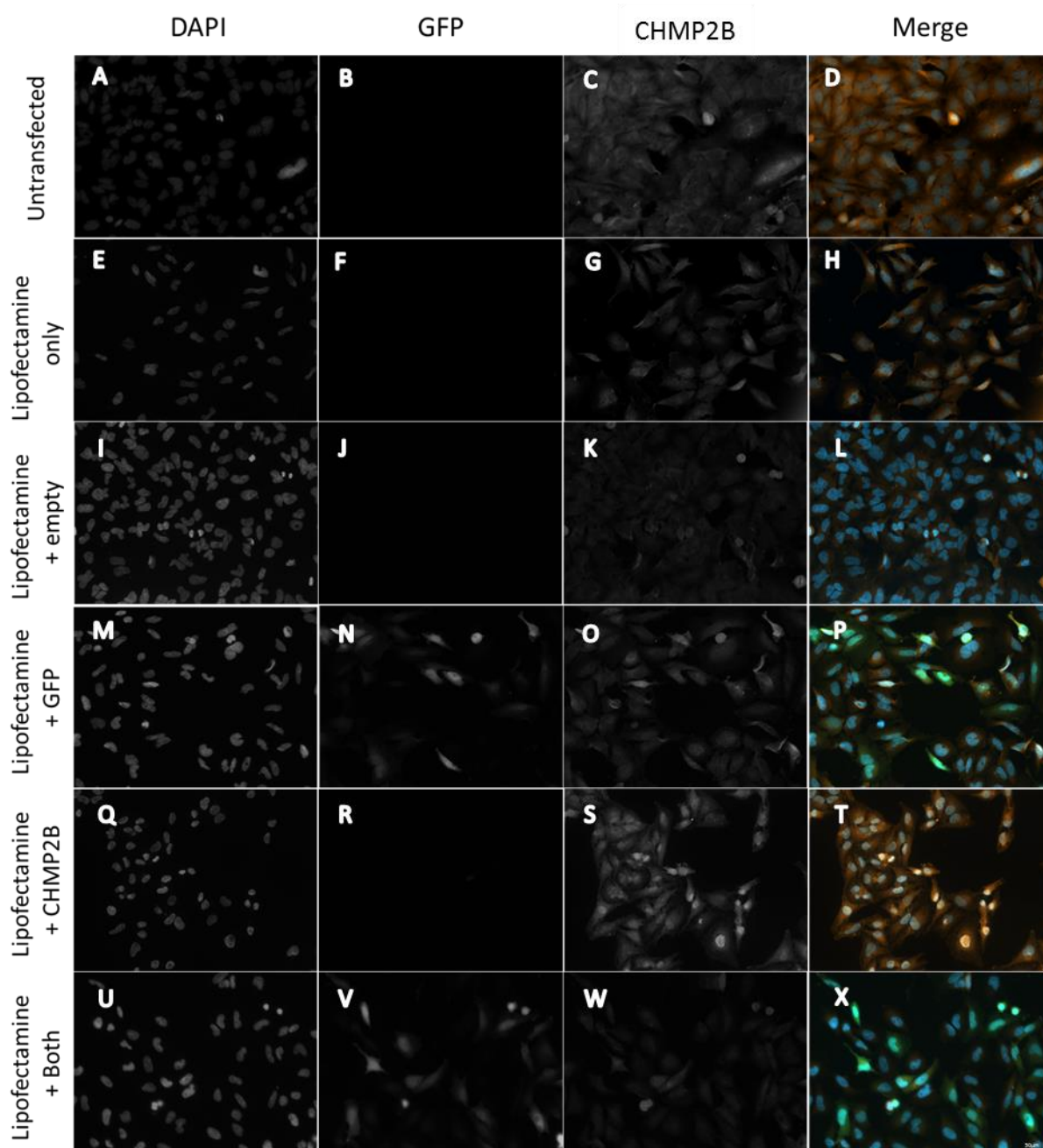
Figure 3.3.1. An expression model was created to investigate the effects of mutant CHMP2B on cellular morphology and localisation in HeLa cells. Controls using unstained cells (A-D), Lipofectamine only (E-H) and Lipofectamine with pBI empty (I-L) were used to compare against conditions with Lipofectamine and pEGFP-C1 (M-P), Lipofectamine and CHMP2BWT (Q-T) and Lipofectamine with both CHMP2BWT and pEGFP-C1 (U-X). Images taken at 20x magnification. Scale bar 50μm

Following transfections in HeLa cells, the same transfections were carried out in 1321N1 cell lines. Untransfected cells were used again as a baseline to compare all other conditions to (Figure 3.3.2 A-D). In the 1321N1 cells the Lipofectamine only control also showed fewer cells than other conditions as was also seen in HeLa cells but were visually the same as the untransfected cells (Figure 3.3.2 E-H). The Lipofectamine plus pBI Empty condition also showed difference to the untransfected cells (Figure 3.3.2 I-L). The Lipofectamine plus pEGFP-C1

condition showed approximately 20% of 1321N1 cells being positive for GFP expression (Figure 3.3.2 M-P). This was much lower than in the HeLa cells. The Lipofectamine plus CHMP2B condition in 1321N1 cells was the same as with the HeLa cells and upon visual inspection looked the same as the untransfected cells (Figure 3.3.2 Q-T). The final condition of Lipofectamine plus pEGFP-C1 and CHMP2BWT showed only approximately 10% of cells being GFP positive in the 1321N1 cell line (Figure 3.3.2 U-X). As staining intensity changes for CHMP2B in either cell line were not readily apparent, quantification of mean pixel density was analysed to test for any differences.
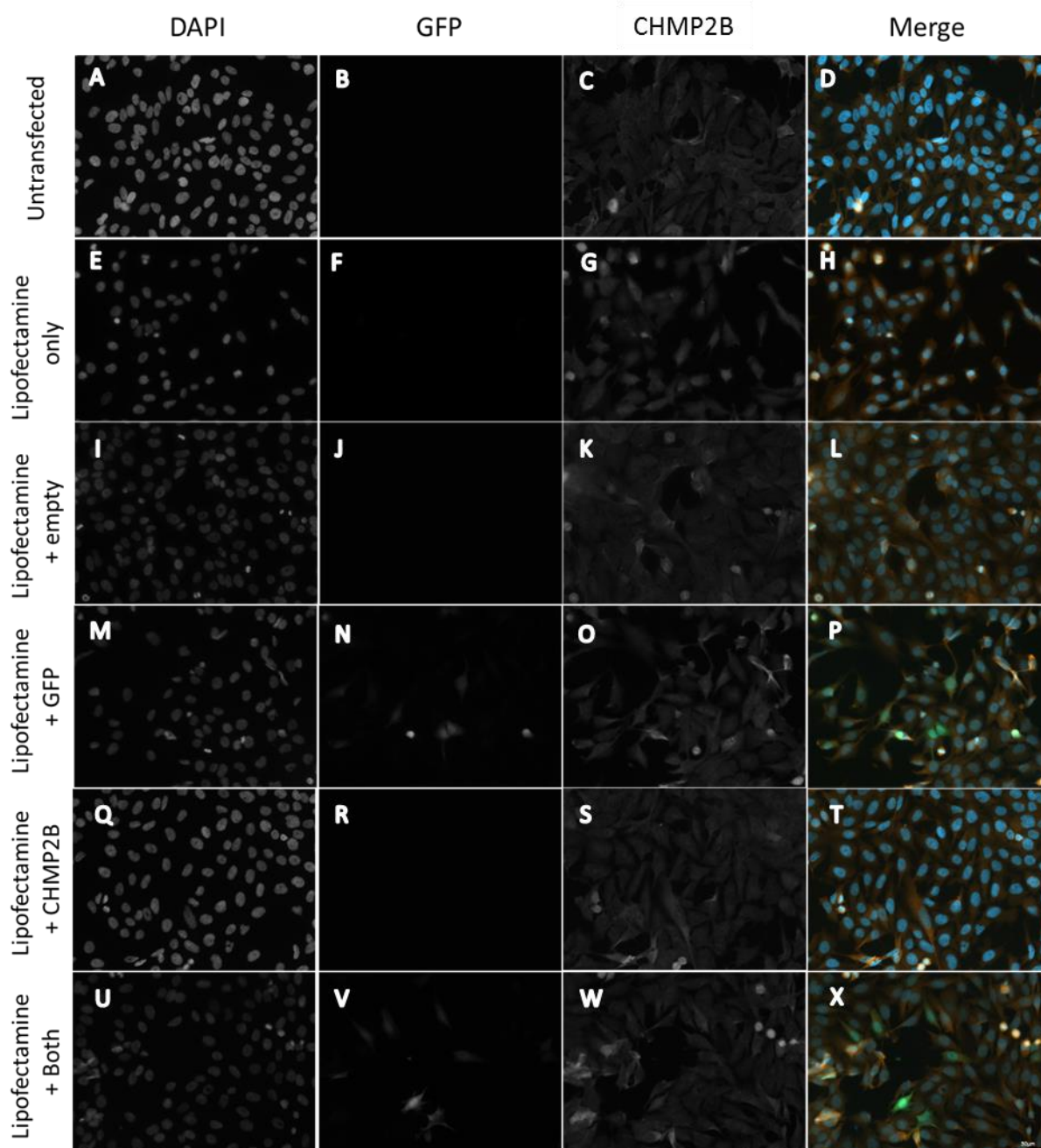
Figure 3.3.2. 1321N1 cells were transfected to create an expression model for investigating the effects of CHMP2B mutants on cellular localisation and morphology. Controls using unstained cells (A-D), Lipofectamine only (E-H) and Lipofectamine with pBI empty (I-L) were used to compare against conditions with Lipofectamine and pEGFP-C1 (M-P), Lipofectamine and CHMP2BWT (Q-T) and Lipofectamine with both CHMP2BWT and pEGFP-C1 (U-X). Images taken at 20x magnification. Scale bar 50µm

The fluorescence intensity of CHMP2B staining in untransfected cells, cells transfected with CHMP2B and cells co-transfected with pEGFP-C1 and CHMP2B were analysed using ImageJ to determine if any increase in CHMP2B could be observed upon transfection. A baseline expression level of CHMP2B fluorescence was determined as the mean intensity of cells in the untransfected controls. All other cell staining intensities were compared to this baseline and

those which varied by more than two standard deviations from this baseline level would be determined to be clearly over-expressing and would be considered successful transfections(Figure 3.3.3). Neither the CHMP2B only transfections, nor CHMP2B and pEGFP-C1 co-transfection produced values above this level. Whether this reflected a high basal expression level of CHMP2B masking the expression of the transfected CHMP2B, whether it suggested a low level of transfection-induced expression or whether the transfection itself failed entirely could not be determined. Given the success of the pEGFP-C1 expression (which is a similarly sized plasmid and uses the same CMV promoter as the CHMP2B expression vector used here), the successful use of this CHMP2B plasmid in the Goldberg lab, the verification of DNA quality by spectrophotometry and agarose gel electrophoresis by other lab members (data not shown) and the well-established use of co-transfection of fluorescent reporters as a means to confirm expression of a gene of interest; the project proceeded on the assumption that GFP+ cells were also expressing CHMP2B WT or mutant, as appropriate.
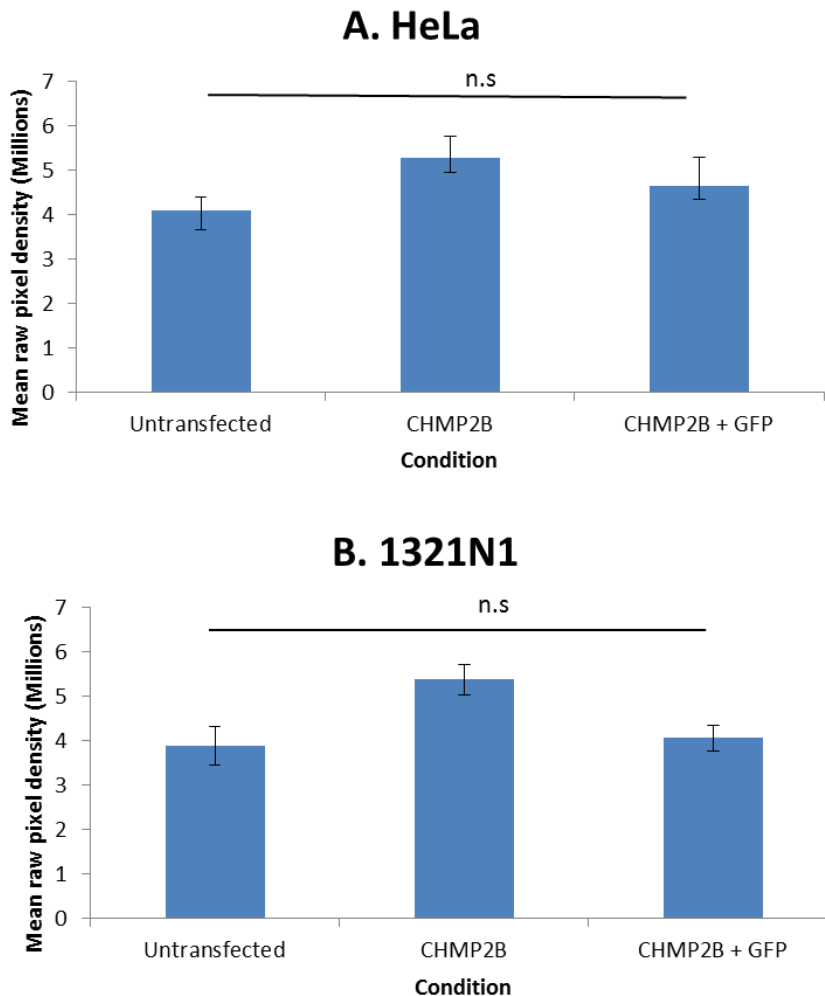
A. HeLa

B. 1321N1

Figure 3.3.3. Fluorescence intensities were measured using imageJ for untransfected, CHMP2B only transfected and CHMP2B and pEGFP-C1 co-transfected cells in order to identify any variance in fluorescence levels of CHMP2B following transfection. For both HeLa (A) and 1321N1 (B) cells no significant difference was found between mean pixel densities as all groups had very high standard deviations. n=10 fields of view. Error bars show SD.

3.4 Analysis of effects of CHMP2B mutants

Cells were transfected using CHMP2BWT and CHMP2BI5 to determine if the expression of the mutant form caused any changes to localisation of CHMP2B and morphology of the cells. When comparing the CHMP2BWT and CHMP2BI5 transfected cells no differences could be observed in cellular morphology in either HeLa cells or 1321N1 cells (Figures 3.4.1 and 3.4.2). No difference was seen when comparing to untransfected cells around them either. Difficulty arose in trying to determine any changes to localisation of CHMP2B due to the high levels of basal expression already seen. No visible differences could be seen in each cell type (Figures 3.4.1 and 3.4.2).
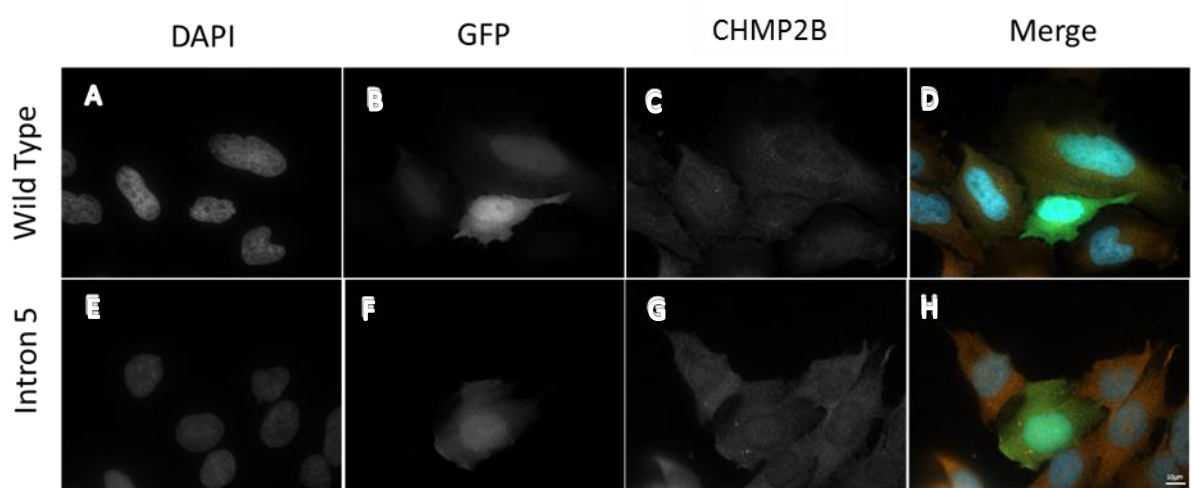
Figure 3.4.1. HeLa cells transfected with CHMP2BWT (A-D) and CHMP2BI5 (A-D) showed no visible changes in morphology or in localisation differences in CHMP2B. Images taken at 63x magnification. Scale bar 10µm.
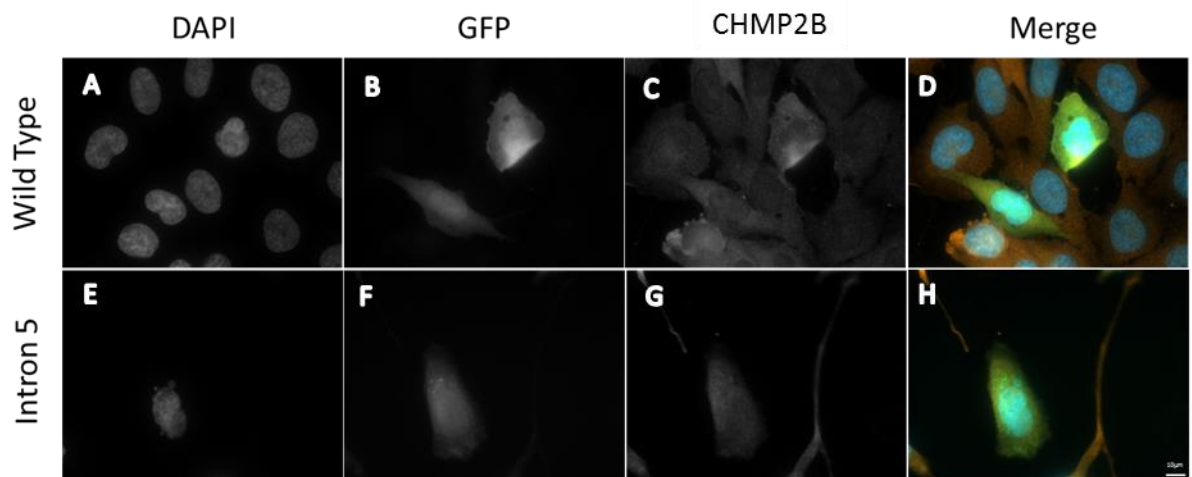

Figure 3.4.2. 1321N1 cells were transfected with CHMP2BWT (A-D) and CHMP2BI5 (A-D) and showed no visible changes in morphology or in localisation in CHMP2B. Images taken at 63x magnification. Scale bar 10µm.

3.5 Semi-functional analysis

3.5.1 Antibody Controls

In order to determine if CHMP2B mutants played a role in altered cellular function the localisation of the glutamate transporters EAAT1 and EAAT2 were investigated. Initially staining controls were conducted to test the validity of the antibody and also allow for visualisation of basal glutamate transporter localisation. EAAT1 was tested first using HeLa cells. Unstained cells were used to compare to which showed no signal in the dsRED channel (Figure 3.5.1.1 A-C). The primary only stain showed no signal in the dsRed channel (Figure 3.5.1.1 D-F), nor did the secondary only (Figure 3.5.1.1. G-I). In the HeLa cells when both

antibodies were applied sequentially there was still no signal in the dsRed channel (Figure 3.5.1.1. J-L). This shows there is no EAAT1 present within HeLa cells.
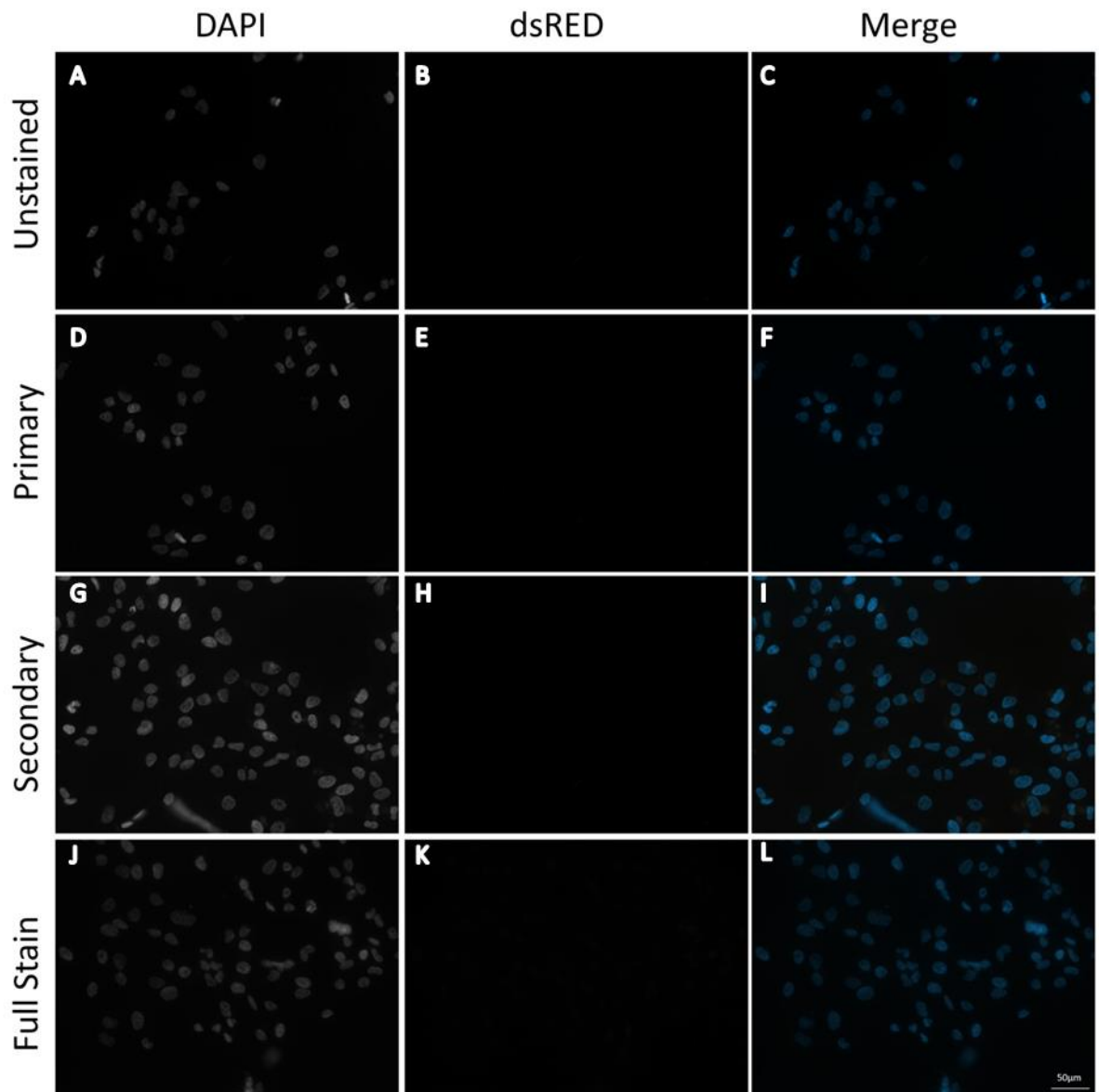

Figure 3.5.1.1. Antibody staining for EAAT1 in HeLa cells. No staining was seen in any condition, even in the full staining. Images taken at 20x magnification. Scale bar 50µm. Example images taken from n=3 slides

The same antibody controls were then conducted for EAAT1 in the astrocytoma cell line 1321N1. Untransfected cells were again used as a control from which to compare other conditions to (Figure 3.5.1.2 A-C). Neither the primary or secondary only stains showed any signal in the dsRed channel (Figure 3.5.1.2 D-F and G-I). In the full stain using both primary and secondary antibody showed positive staining for EAAT1 in all cells (Figure 3.5.1.2 J-L).
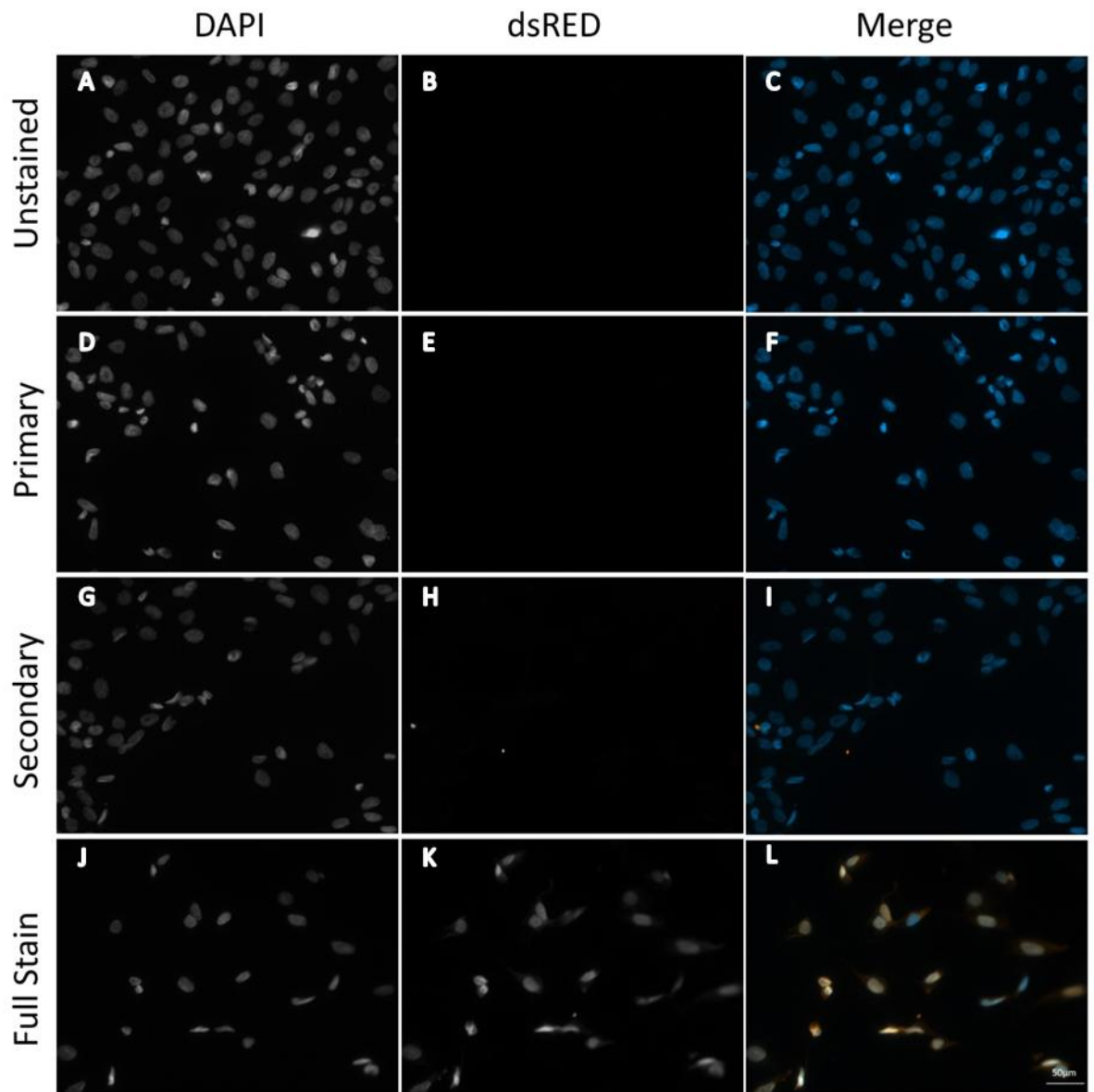
Figure 3.5.1.2. Antibody staining for EAAT1 in 1321N1 cells. No cell staining was seen in either the primary (D-F) or secondary (G-I) conditions and looked identical to the unstained cells (A-C). In the full stain condition (J-L) staining was seen in all cells. Images were taken at 20x magnification. Scale bar 50μm. Example images from n=3 slides

Staining controls were the conducted for EAAT2 in HeLa cells. Unstained cells showed no signal in the dsRED channel and were used to compare to (Figure 3.5.1.3 A-C). No staining was seen when either primary alone or secondary antibody alone were used (Figure 3.5.1.2 D-F and G-I). There was also no staining observed in HeLa cells when application of both antibodies also showing EAAT2 is not expressed in HeLa cells (Figure 3.5.1.3 J-L).
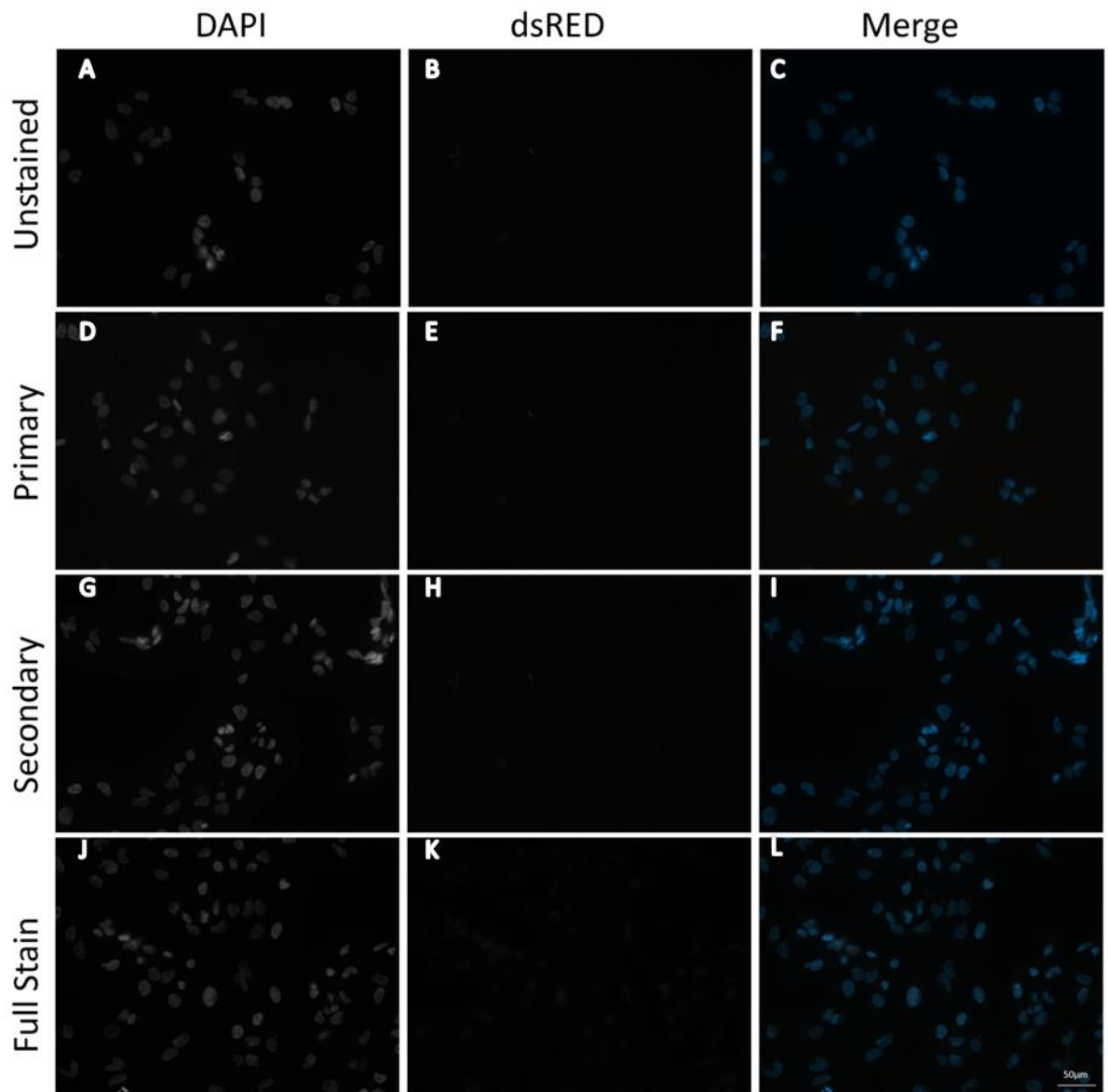
Figure 3.5.1.3. Antibody staining for EAAT2 in HeLa cells showed no staining in any condition and were indistinguishable from the unstained cells. Images were taken at 20x magnification. Scale bar 50µm. Example images from n=3 slides

Finally the EAAT2 antibody was also tested in 1321N1 cell lines. Untransfected cells showed no signal in the dsRED channel (Figure 3.5.1.4 A-C). Both primary only and secondary only also showed no signal in the dsRED channel and were visually identical to the untransfected cells (Figure 3.5.1.3 D-F and G-I). Finally sequential used of the primary followed by the secondary antibody showed all cells stained positive for EAAT2 in 1321N1 cell lines (Figure 3.5.1.4 J-L).
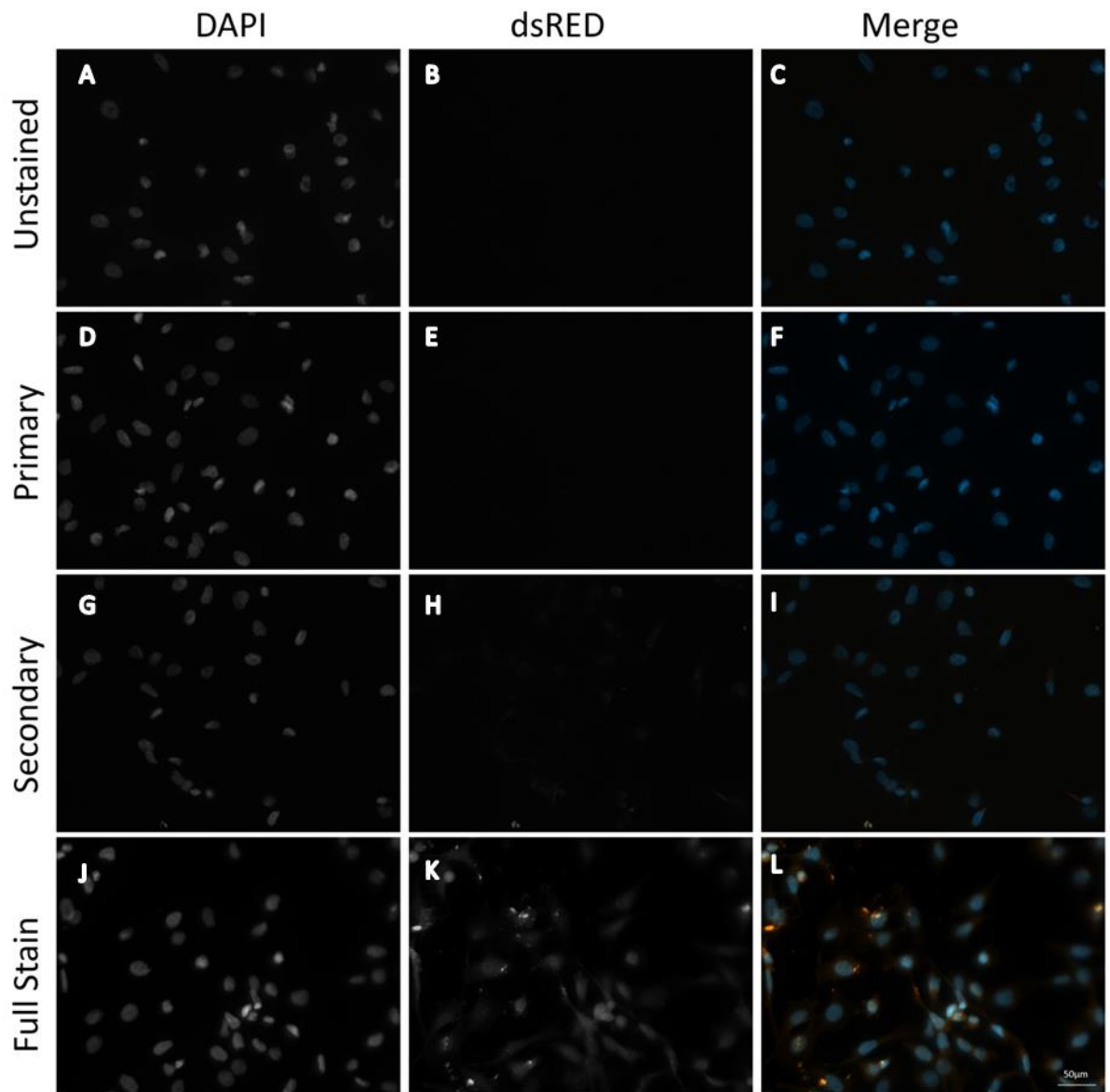
Figure 3.5.1.4. Antibody staining for EAAT2 in 1321N1 cells. Both the primary only (D-F) and secondary only (G-I) conditions were visually identical to the unstained cells. In the full stain condition (J-L) staining was seen in all cells. Images were taken at 20x magnification. Scale bar 50μm. Example images from n=3 slides

High magnification images were taken of EAAT1 and EAAT2 staining in 1321N1 cell lines to determine normal localisation patterns within the cells (Figure 3.5.1.5). EAAT1 appeared to be present throughout the cell (Figure 3.5.1.5 A-C). EAAT2 also appeared to be expressed throughout the cells but there appeared to be a slightly higher density surrounding the nucleus. (Figure 3.5.1.5 D-F). Since HeLa cells did not contain any EAAT1 or EAAT2 only 1321N1 cells were used for subsequent experiments.

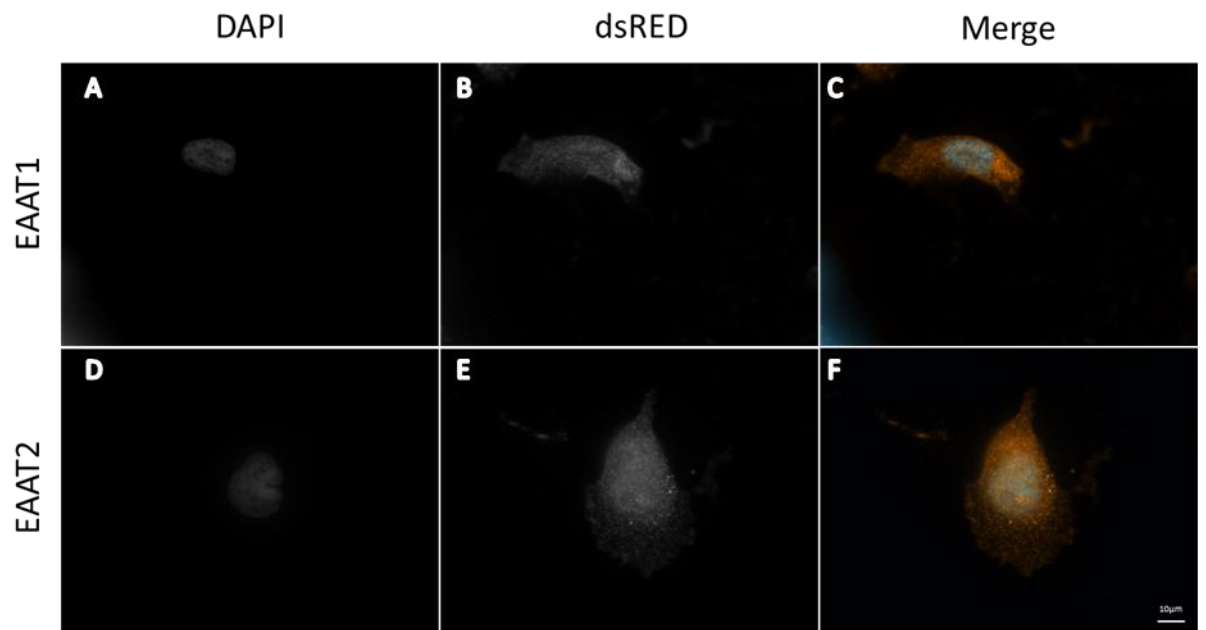Figure 3.5.1.5. High magnification images of basal EAAT1 (A-C) and EAAT2 (D-F) expression in untransfected 1321N1 cells. Images taken at 63x magnification. Scale bar 10µm. Example images from n=3 slides

3.5.2 Analysis of Localisation

1321N1 cells were transfected with CHMP2BWT and CHMP2BI5 to determine if CHMP2B mutants had any effects on the localisation of EAATs within the cells. Firstly comparisons were made between with type and mutant transfected cells stained for EAAT1 (Figure 3.5.2.1). No differences were observed between the wild type (Figure 3.5.2.1 A-C) and the mutant transfected cells (Figure 3.5.2.1 D-F).

Figure 3.5.2.1. 1321N1 cells were transfected with CHMP2BWT (A-D) and CHMP2BI5 (E-H) and stained using anti-EAAT1 antibody. Images were taken at 63x magnification. Scale bar 10µm. Example images from n=3 slides

The same was then repeated for EAAT2 (Figure 3.5.2.2). There was also no visible difference between the wild type (Figure 3.5.2.2 A-C) and mutant transfected cells (Figure 3.5.2.2 D-F).
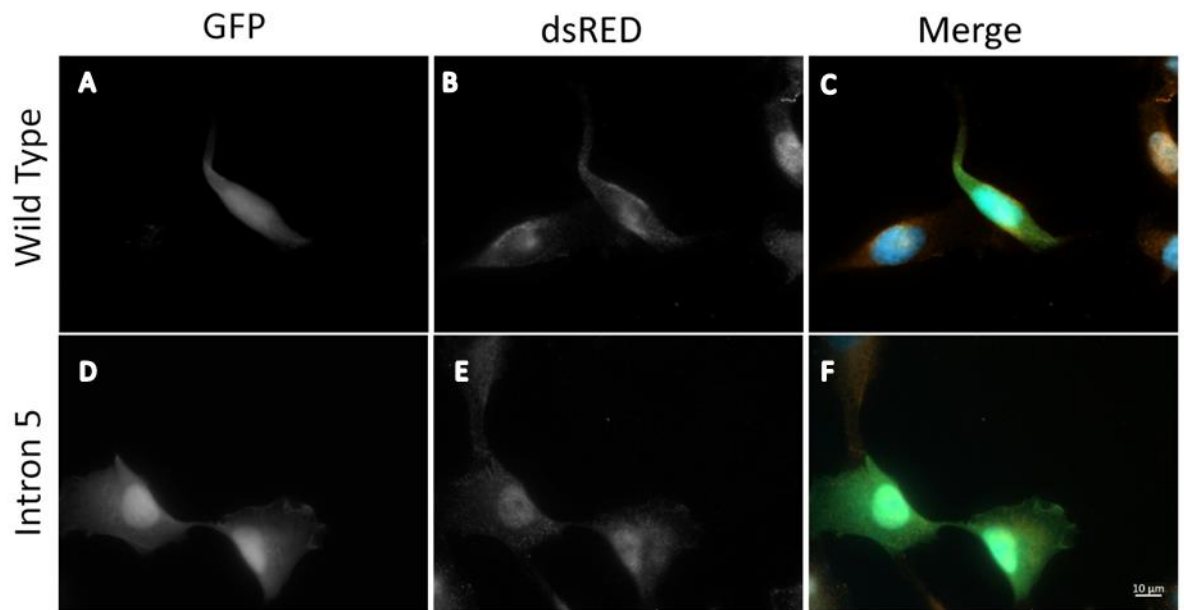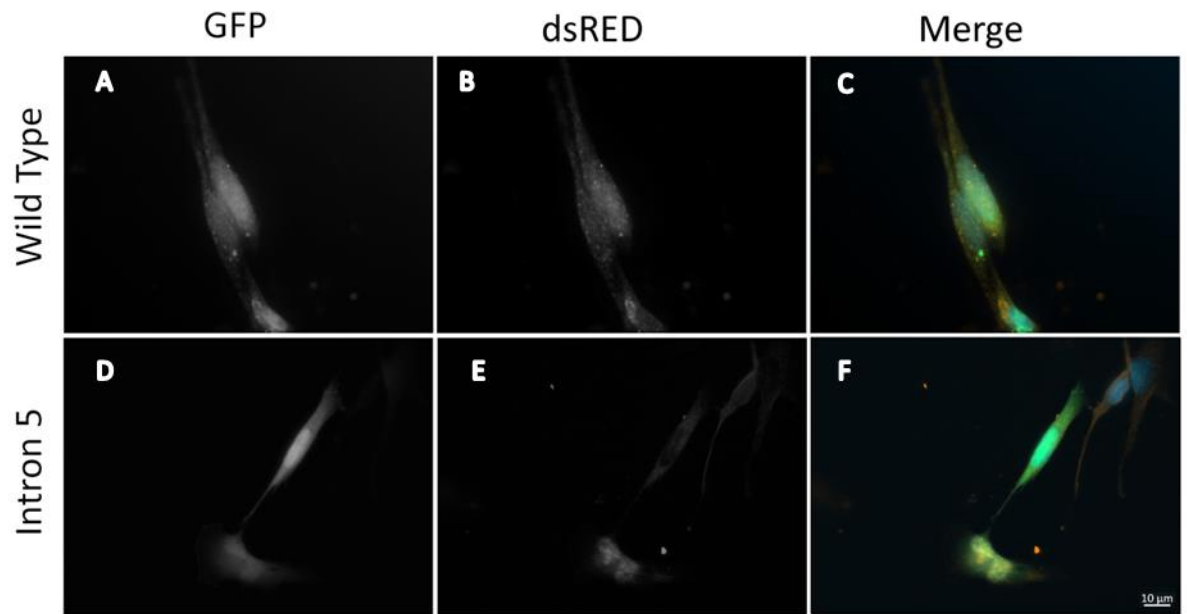
Figure 3.5.2.2. 1321N1 cells were transfected with CHMP2BWT (A-D) and CHMP2BI5 (E-H) and stained using anti-EAAT2 antibody. Images were taken at 63x magnification. Scale bar 10μm. Example images from n=3 slides

4. Discussion

Mutations in the ESCRT-III complex protein CHMP2B have been implicated in a variety of neurodegenerative diseases and are known to produce a rare familial form of frontotemporal dementia (Yamazaki *et al.*, 2010; Isaacs *et al.*, 2011). All other previous research has investigated either how these disease causing mutations in CHMP2B affect either neurons or the brain as a whole, but none have looked at CHMP2B in astrocytes despite astrocytes being implicated in virtually every neuropathology including frontotemporal dementia (Hallmann *et al.*, 2017). Accordingly, this project aimed to carry out some initial investigations of CHMP2B in astrocytes; namely to confirm basal expression of the protein CHMP2B in astrocytes and determine what affect the FTD-associated mutation CHMP2B Intron 5 has on basic astrocyte biology, as indicated by cellular morphology and glutamate transporter localisation.

4.1 Confirmation of CHMP2B expression in astrocytes

While it has been previously suggested that CHMP2B is ubiquitously expressed throughout the body (Chassefeyre *et al.*, 2015), no published research has ever explicitly investigated its expression in astrocytes. In order to confirm basal expression this project began by western blotting and immunofluorescence staining to elucidate basal expression and staining patterns in astrocytes.

Confirmation of CHMP2B in astrocytes was achieved by western blotting using cell lysates. The western blot produced bands of approximately 25kDa which corresponds with the predicted molecular weight of CHMP2B in all cell types tested, including the astrocyte cell line 1321N1 and normal human astrocytes (NHA). The protein band size observed in this project is consistent with other research using the same anti-CHMP2B antibody hence this is likely to be accurate (Belly *et al.*, 2010; Ghazi-Noori *et al.*, 2012). As previously stated, CHMP2B is already known to be expressed in HeLa cells (Atilla-Gokcumen *et al.*, 2014) so they were used in this project as a positive control and yielded a band of identical weight to that seen in the 1321N1 or NHA cells. Taken together, these data confirm that CHMP2B is indeed expressed in human astrocytes.

A BCA assay was conducted prior to western blotting to determine protein concentration in cell lysates and to ensure equal protein loading in each lane. However, the intensity of the loading control band (beta actin) was seen to be much lower in the HeLa cells than in the 1321N1 cells and NHAs. This indicates that the lanes were unequally loaded as beta actin is a constitutively expressed protein so all bands should have been equal (Taylor *et al.*, 2013). One possible cause for this loading inconsistency could be due to the choice of protein assay. It has

been reported that certain factors can alter the accuracy of the BCA assay, including protein composition, post-translational modifications and interfering substances which may be present (Brady and Macnaughtan, 2015). The BCA assay was chosen due to its compatibility with the detergent-containing RIPA lysis buffer, however for future work an alternative assay, such as the Bradford assay, in combination with a compatible lysis buffer.

Another potential explanation for the loading inconsistencies may have been degradation of the lysates following BCA assay due to freeze-thaw effects, as the BCA was conducted prior to initial freezing of the lysates. For any future work it would be better to conduct a BCA assay on the defrosted lysates immediately prior to running the blot to ensure protein concentrations at the time are being measured.

Densitometry was conducted on the bands in order to normalise the CHMP2B concentration in each lane relative to beta actin in a semi-quantitative manner and permit the estimation of relative CHMP2B expression in each cell type, taking into account the inconsistent protein loading. Densitometry has been reported to be a reliable method for quantification of western blot data as opposed to visual inspection the blot (Taylor *et al.*, 2013). Densitometry suggested that the HeLa had the highest relative CHMP2B expression whilst the normal human astrocytes had the lowest. Unfortunately, due to inconsistent blot quality densitometry could only be carried out on one single blot, so full conclusions regarding relative expression levels were not possible. If these results are validated then it could imply that astrocytes express a higher level of CHMP2B than non-glial cells. It has been reported that ESCRTs are required for the formation of exosomes via MVB formation (Verkhratsky *et al.*, 2016). Since astrocytes are vital for release and uptake of glutamate at synapses, this could imply a greater need for CHMP2B and ESCRTs in astrocytes.

Immunofluorescence staining of cell lines with an anti-CHMP2B antibody was conducted to visually confirm basal expression of CHMP2B in astrocytes and identify any specific localisation patterns within cells. High levels of staining were present in both 1321N1 and HeLa cell types and was seen to extend throughout the cell in a punctate manner. The staining pattern observed was similar to that seen in another study which had utilised this antibody in neurons (Bodon *et al.*, 2011). This result provides further confirmation that CHMP2B is expressed in astrocytes, as 1321N1 cells are derived from astrocytoma tissue. ImageJ was used to analyse the fluorescence intensities of the CHMP2B in the two cell lines which showed no significant difference. This result roughly corresponds with that observed with the densitometry, where 1321N1 and HeLa cell lysate CHMP2B band densities were similar (although statistical analysis was not possible). Normal human astrocytes were unavailable for this and the subsequent

stages of this project due to a range of factors including inconsistent supply and manufacturer media shortages. This can be a common issue when using primary human cells, whose availability depends on human donation as a by-product of biopsies and which utilise extremely defined medium compositions. Based upon the densitometry data, it would not be unexpected that NHAs would have higher fluorescence levels than the cell lines, but this should form the basis of further studies.

4.2. Creation of expression model

In order to transiently express wild-type and mutant CHMP2B in cells to assess their relative effects on phenotype, an expression model was created using the transfection reagent Lipofectamine 3000. Lipofectamine reagents have become some of the most widely used transfection reagents and are considered the gold standard for transfection reagent (Cardarelli *et al.*, 2016). Prior to the project different transfection methods had been tested in the lab and Lipofectamine 3000 was deemed to be the most effective method for astrocyte transfections (Dr Vicky Jones, personal communication). The "Lipofection" method works by DNA, which is negatively charged, being contained within cationic liposomes which are formed by the Lipofectamine reagent. These DNA-loaded liposomes then fuse with the cell membrane which allows for the release of the DNA into the cell (Balazs and Godbey, 2011; Sandbichler *et al.*, 2013). If DNA encoding different proteins are mixed, in this case pEGFP-C1 and CHMP2B, the liposomes should take up both DNAs and both would be released into the cell. This technique has been used widely as a means to co-express a gene of interest alongside a reporter gene, such as a fluorescent protein, in many cell types including astrocytes (Montana *et al.*, 2004; Ni and Parpura, 2009; Malarkey and Parpura, 2011). Hence, it was reasonable to assume that cells which were positive for GFP in the co-transfected experiments would also be positive for CHMP2B.

To first optimise the single transfection protocol, different ratios of plasmid DNA (pEGFP-C1) and lipofectamine reagent were compared to determine which provided the highest transfection efficiencies (as measured by the number of GFP+ cells).

 For the HeLa cells a greater difference in transfection efficiency was seen when a higher amount of DNA was used but not when a higher volume of lipofectamine was used. In 1321N1 cells a higher volume of lipofectamine increased the transfection efficiency but a higher DNA volume did not increase efficiency. Generally, 1321N1 cells produced much lower GFP positive cells compared to HeLa cells. This was also the case when co-transfecting which were lower for both cell types when compared to the single transfection.

Increasing of both DNA and Lipofectamine reagent increased the transfection efficiencies in both cell types. This is likely to be due to a higher number of liposome complexes containing more DNA being formed and therefore a greater chance of the DNA being internalised by the cells. While HeLa transfections reached a consistent level of around 70%, in 1321N1 cells transfection efficiencies remained low at around 20%. This would be expected as all brain cell types, astrocytes included, have been reported to be somewhat hard to transfect (Marucci *et al.*, 2011).. The confluency of cells and overall cellular morphology following transfection was also investigated as a measure of cellular toxicity mediated by the transfection reagent. No significant difference was seen in either case upon any treatment, suggesting that the Lipofectamine had no toxic effect on the cells tested and was suitable for use in the planned experiments.

4.3 Analysis of effects of CHMP2B mutants

This project aimed to determine if a mutant form of CHMP2B affected the cellular morphology of astrocytes. When the transfection protocol had been optimised cells were either transfected with plasmids encoding wild-type CHMP2B (CHMP2BWT) or plasmids encoding the most common FTD causing mutant variant of CHMP2B, the truncated CHMP2B intron 5 variant (CHMP2BI5) (van der Zee *et al.*, 2008; Belly *et al.*, 2010). When comparing cells transfected with CHMP2BWT and those transfected with the mutant form CHMP2BI5, no differences were noted in astrocyte morphology – a phenomenon which is increasingly being linked with neurodegenerative disorders (Olabarria *et al.*, 2010; Jones *et al.*, 2017). Similarly, no obvious alteration in the localisation of CHMP2B as observed upon expression of the intron 5 variant; however it was difficult to visualise transiently expressed CHMP2B above basal expression. One paper which looked at the effects of CHMP2B mutations in neurons noted that the mutant CHMP2B which was stained using an anti-tag antibody formed clusters and aggregates unlike the WT form (Belly *et al.*, 2010). It was impossible to differentiate between endogenously expressed and transiently expressed CHMP2B in this project as the CHMP2B plasmids available did not contain a specific tag which could have been used to detect the transfected CHMP2B only. Another plasmid containing CHMP2B with a FLAG tag was received from Y. Goldberg towards the end of the project which would be useful for any future research into CHMP2B, however it was too late to use during this project. Use of an anti-FLAG antibody would allow for differentiation between basal CHMP2B and transfected (FLAG-tagged) CHMP2B, as has been carried out elsewhere (Bodon *et al.*, 2011; Cheruiyot *et al.*, 2014).

The morphology of astrocytes is vital to their functioning within the brain. Reactive gliosis is the process by which astrocytes change their shape and size in response to central nervous

system damage (Burda and Sofroniew, 2014). Reactive gliosis has been observed in neurodegenerative disorders previously and it was conceivable that introduction of the FTD-causing CHMP2BIB mutant could cause a change in cell morphology (Verkhratsky *et al.*, 2014; Pekny and Pekna, 2016). No changes to either astrocyte (1321N1) or HeLa morphology were observed in this research. This could either be due to the CHMP2B intron 5 mutant having no effect on astrocyte morphology or due to experimental limitations. For example, it was hard to differentiate between transfected and non-transfected cells using the anti-CHMP2B antibody alone. This could be explained by the relatively high basal expression levels masking additional transient expression, or may be due to relatively poor levels of overexpression in the transfected cells caused by, for example, not enough DNA being transfected into the cells, as it was known the transfection levels were extremely low within the 1321N1 cell lines. There may have been issues already within the cells which may have affected the CHMP2B plasmid expression (e.g. underlying infection) or that the cells may already exhibit a changed shape because they are derived from an astrocytoma, rather than normal cells.

The glutamate transporters EAAT1 and EAAT2 are responsible for the uptake of over 95% of glutamate in the brain and their availability is vital for normal functioning of astrocytes. Staining for the glutamate transporters EAAT1 and EAAT2 were conducted in both HeLa cells and 1321N1 cells. As expected the results showed no staining for either transporter in HeLa cells, as these are brain specific transporters (Ugbode *et al.*, 2017) . Comparisons showed no differences in EAAT1 or EAAT2 localisation in the 1321N1 cells when expressing CHMP2BI5 compared to WT. This could imply that the CHMP2B Intron 5 mutation is not implicated in astrocyte glutamate handling and/or may not be linked to localisation of these transporters. Alternatively, as outlined above, it may be that the levels of expression were not sufficient to induce any changes.

Project limitations

During this project, frequent issues were experienced with transfecting the cell lines and it was only in the final few months of the project that the transfections began working. There were consistent issues regarding infection in the communal lab for the duration of the project and also there were problems with regards to DNA quality which set the project back. Freeze-thawing of the plasmid DNA may have caused degradation and therefore it is possible that not enough intact plasmid DNA was being added to the transfection mix which could account for some of the transfection problems seen within this project.

Transfections remained difficult with the 1321N1 cell line, which have been reported to be particularly difficult to transfect (Marucci *et al.*, 2011). The highest transfection efficiencies

achieved in this cell line was only 22% but this decreased to an average of 12% when attempting co-transfections using both CHMP2B and pEGFP-C1. HeLa cells were found to be much easier to transfect than 1321N1 cells and showed transfection efficiencies of over 70% when only transfecting pEGFP-C1 and this decreased to 40% when co-transfecting.

Due to the length of the project, the low transfection levels were considered to be manageable as most of the project was immunofluorescence based and it was not essential that a large proportion of cells would need to be expressing the desired protein as would have been the case for functional analysis. It is a possibility that the lack of any differences observed in this project could be due to the amount of DNA being transfected not being enough to have a significant effect due to the high basal levels of CHMP2B.

4.4 Future Works

Whilst this research did not find any conclusive results in regards to how CHMP2B mutations may affect astrocyte morphology or glutamate transporter localisation it has identified that CHMP2B is expressed in astrocytes. No other research has shown this previously and this opens up a new area of research opportunity in regards to how CHMP2B may play a role in neurodegeneration via astrocyte pathology.

Further research should aim to confirm robust expression of transfected CHMP2B using a plasmid containing a FLAG tag and anti-FLAG antibody to identify transfected CHMP2B as opposed to basal CHMP2B. This would allow for confirmation of transfection without the need for GFP, allow for localisation differences between WT and I5 to be assessed and permit clear conclusions to be drawn.

Other future work should aim to begin investigating if CHMP2B mutants that have been seen to produce FTD also affect astrocytes in similar ways to neurons. Previous research has already elucidated some effects in neurons but moving forward the effects of mutant CHMP2B in astrocytes needs to be investigated. One potential route of investigation could be to compare levels of CHMP2B in neurons and astrocytes. It was seen in this project that astrocytes appear to express a high basal level of CHMP2B; it would be interesting to compare this to both neurons and other glial cells such as microglia which may also play a role in neurodegeneration during FTD as this could indicate astrocytes may play more of a role in disease progression than is currently thought.

References

Alonso Y Adell, M. and Teis, D. (2011) 'Assembly and disassembly of the ESCRT-III membrane scission complex', *FEBS Letters*, pp. 3191–3196. doi: 10.1016/j.febslet.2011.09.001.

Atilla-Gokcumen, G. E., Muro, E., Relat-Goberna, J., Sasse, S., Bedigian, A., Coughlin, M. L., Garcia-Manyes, S. and Eggert, U. S. (2014) 'Dividing cells regulate their lipid composition and localization.', *Cell*. Elsevier, 156(3), pp. 428–39. doi: 10.1016/j.cell.2013.12.015.

Babst, M., Katzmann, D. J., Estepa-Sabal, E. J., Meerloo, T. and Emr, S. D. (2002) 'Escrt-III: An Endosome-Associated Heterooligomeric Protein Complex Required for MVB Sorting', *Developmental Cell*, 3(2), pp. 271–282. doi: 10.1016/S1534-5807(02)00220-4.

Balazs, D. A. and Godbey, W. (2011) 'Liposomes for use in gene delivery.', *Journal of drug delivery*. Hindawi, 2011, p. 326497. doi: 10.1155/2011/326497.

Belly, A., Bodon, G., Blot, B., Bouron, A., Sadoul, R. and Goldberg, Y. (2010) 'CHMP2B mutants linked to frontotemporal dementia impair maturation of dendritic spines.', *Journal of cell science*. Inserm, 123(Pt 17), pp. 2943–54. doi: 10.1242/jcs.068817.

Bodon, G., Chassefeyre, R., Pernet-Gallay, K., Martinelli, N., Effantin, G., Hulsik, D. L., Belly, A., Goldberg, Y., Chatellard-Causse, C., Blot, B., Schoehn, G., Weissenhorn, W. and Sadoul, R. (2011) 'Charged multivesicular body protein 2B (CHMP2B) of the endosomal sorting complex required for transport-III (ESCRT-III) polymerizes into helical structures deforming the plasma membrane.', *The Journal of biological chemistry*. American Society for Biochemistry and Molecular Biology, 286(46), pp. 40276–86. doi: 10.1074/jbc.M111.283671.

Brady, P. N. and Macnaughtan, M. A. (2015) 'Evaluation of colorimetric assays for analyzing reductively methylated proteins: Biases and mechanistic insights.', *Analytical biochemistry*. NIH Public Access, 491, pp. 43–51. doi: 10.1016/j.ab.2015.08.027.

Brettschneider, J., Libon, D. J., Toledo, J. B., Xie, S. X., McCluskey, L., Elman, L., Geser, F., Lee, V. M.-Y., Grossman, M. and Trojanowski, J. Q. (2012) 'Microglial activation and TDP-43 pathology correlate with executive dysfunction in amyotrophic lateral sclerosis', *Acta Neuropathologica*, 123(3), pp. 395–407. doi: 10.1007/s00401-011-0932-x.

Burda, J. E. and Sofroniew, M. V (2014) 'Reactive gliosis and the multicellular response to CNS damage and disease.', *Neuron*. NIH Public Access, 81(2), pp. 229–48. doi: 10.1016/j.neuron.2013.12.034.

Cardarelli, F., Digiacomo, L., Marchini, C., Amici, A., Salomone, F., Fiume, G., Rossetta, A., Gratton, E., Pozzi, D. and Caracciolo, G. (2016) 'The intracellular trafficking mechanism of Lipofectamine-based transfection reagents and its implication for gene delivery', *Scientific Reports*. Nature Publishing Group, 6(1), p. 25879. doi: 10.1038/srep25879.

Cassano, T., Serviddio, G., Gaetani, S., Romano, A., Dipasquale, P., Cianci, S., Bellanti, F., Laconca, L., Romano, A. D., Padalino, I., LaFerla, F. M., Nicoletti, F., Cuomo, V. and Vendemiale, G. (2012) 'Glutamatergic alterations and mitochondrial impairment in a murine model of Alzheimer disease', *Neurobiology of Aging*, 33(6), p. 1121.e1-1121.e12. doi: 10.1016/j.neurobiolaging.2011.09.021.

Chassefeyre, R., Martínez-Hernández, J., Bertaso, F., Bouquier, N., Blot, B., Laporte, M., Fraboulet, S., Couté, Y., Devoy, A., Isaacs, A. M., Pernet-Gallay, K., Sadoul, R., Fagni, L. and Goldberg, Y. (2015) 'Regulation of postsynaptic function by the dementia-related ESCRT-III subunit CHMP2B.', *The Journal of neuroscience : the official journal of the Society for Neuroscience*, 35(7), pp. 3155–73. doi: 10.1523/JNEUROSCI.0586-14.2015.

Chen, S., Sayana, P., Zhang, X. and Le, W. (2013) 'Genetics of amyotrophic lateral sclerosis: an update', *Molecular Neurodegeneration*. BioMed Central, 8(1), p. 28. doi: 10.1186/1750-1326-8-28.

Cheruiyot, A., Lee, J.-A., Gao, F.-B. and Ahmad, S. T. (2014) 'Expression of mutant CHMP2B, an ESCRT-III component involved in frontotemporal dementia, causes eye deformities due to Notch misregulation in Drosophila.', *FASEB journal : official publication of the Federation of American Societies for Experimental Biology*. The Federation of American Societies for Experimental Biology, 28(2), pp. 667–75. doi: 10.1096/fj.13-234138.

Choi, S. H., Veeraraghavalu, K., Lazarov, O., Marler, S., Ransohoff, R. M., Ramirez, J. M. and Sisodia, S. S. (2008) 'Non-Cell-Autonomous Effects of Presenilin 1 Variants on Enrichment-Mediated Hippocampal Progenitor Cell Proliferation and Differentiation', *Neuron*, 59(4), pp. 568–580. doi: 10.1016/j.neuron.2008.07.033.

Clare, R., King, V. G., Wirenfeldt, M. and Vinters, H. V (2010) 'Synapse loss in dementias.', *Journal of neuroscience research*. NIH Public Access, 88(10), pp. 2083–90. doi: 10.1002/jnr.22392.

Clayton, E. L., Mizielinska, S., Edgar, J. R., Nielsen, T. T., Marshall, S., Norona, F. E., Robbins, M., Damirji, H., Holm, I. E., Johannsen, P., Nielsen, J. E., Asante, E. A., Collinge, J., The Freja Consortium and Isaacs, A. M. (2015) 'Frontotemporal dementia caused by CHMP2B mutation is

characterised by neuronal lysosomal storage pathology', *Acta Neuropathologica*. doi: 10.1007/s00401-015-1475-3.

Cosker, K. E. and Segal, R. A. (2014) 'Neuronal signaling through endocytosis', *Cold Spring Harbor Perspectives in Biology*. Cold Spring Harbor Laboratory Press, 6(2). doi: 10.1101/cshperspect.a020669.

Davies, B. A., Azmi, I. F. and Katzmann, D. J. (2009) 'Regulation of Vps4 ATPase activity by ESCRT-III.', *Biochemical Society transactions*, 37(Pt 1), pp. 143–5. doi: 10.1042/BST0370143.

Fahlke, C., Kortzak, D. and Machtens, J.-P. (2016) 'Molecular physiology of EAAT anion channels', *Pflügers Archiv - European Journal of Physiology*. Springer Berlin Heidelberg, 468(3), pp. 491–502. doi: 10.1007/s00424-015-1768-3.

Ferrari, R., Kapogiannis, D., Huey, E. D., Grafman, J., Hardy, J. and Momeni, P. (2010) 'Novel missense mutation in charged multivesicular body protein 2B in a patient with frontotemporal dementia', *Alzheimer Disease and Associated Disorders*, 24(4), pp. 397–401. doi: 10.1097/WAD.0b013e3181df20c7.

Ferrari, R., Kapogiannis, D., Huey, E. D. and Momeni, P. (2011) 'FTD and ALS: a tale of two diseases.', *Current Alzheimer research*. NIH Public Access, 8(3), pp. 273–94. Available at: http://www.ncbi.nlm.nih.gov/pubmed/21222600 (Accessed: 30 August 2017).

Frake, R. A., Ricketts, T., Menzies, F. M. and Rubinsztein, D. C. (2015) 'Autophagy and neurodegeneration', *Journal of Clinical Investigation*, pp. 65–74. doi: 10.1172/JCI73944.

Funk, K. E., Mrak, R. E. and Kuret, J. (2011) 'Granulovacuolar degeneration (GVD) bodies of Alzheimer's disease (AD) resemble late-stage autophagic organelles', *Neuropathology and Applied Neurobiology*, 37(3), pp. 295–306. doi: 10.1111/j.1365-2990.2010.01135.x.

Ghazi-Noori, S., Froud, K. E., Mizielinska, S., Powell, C., Smidak, M., Fernandez De Marco, M., O'Malley, C., Farmer, M., Parkinson, N., Fisher, E. M. C., Asante, E. A., Brandner, S., Collinge, J. and Isaacs, A. M. (2012) 'Progressive neuronal inclusion formation and axonal degeneration in CHMP2B mutant transgenic mice', *Brain*, 135(3), pp. 819–832. doi: 10.1093/brain/aws006.

Di Giorgio, F. P., Carrasco, M. A., Siao, M. C., Maniatis, T. and Eggan, K. (2007) 'Non–cell autonomous effect of glia on motor neurons in an embryonic stem cell–based ALS model', *Nature Neuroscience*. NIH Public Access, 10(5), pp. 608–614. doi: 10.1038/nn1885.

Goedert, M., Ghetti, B. and Spillantini, M. G. (2012) 'Frontotemporal dementia: Implications for understanding Alzheimer disease', *Cold Spring Harbor Perspectives in Medicine*, 2(2), pp. 1–

21. doi: 10.1101/cshperspect.a006254.

Hallmann, A.-L., Araúzo-Bravo, M. J., Mavrommatis, L., Ehrlich, M., Röpke, A., Brockhaus, J., Missler, M., Sterneckert, J., Schöler, H. R., Kuhlmann, T., Zaehres, H. and Hargus, G. (2017) 'Astrocyte pathology in a human neural stem cell model of frontotemporal dementia caused by mutant TAU protein', *Scientific Reports*, 7, p. 42991. doi: 10.1038/srep42991.

Han, X., Yang, L., Du, H., Sun, Q., Wang, X., Cong, L., Liu, X., Yin, L., Li, S. and Du, Y. (2016) 'Insulin Attenuates Beta-Amyloid-Associated Insulin/Akt/EAAT Signaling Perturbations in Human Astrocytes.', *Cellular and molecular neurobiology*. NIH Public Access, 36(6), pp. 851–64. doi: 10.1007/s10571-015-0268-5.

Henne, W. M., Buchkovich, N. J. and Emr, S. D. (2011) 'The ESCRT Pathway', *Developmental Cell*. Elsevier Inc., 21(1), pp. 77–91. doi: 10.1016/j.devcel.2011.05.015.

Hurley, J. H. (2010) 'The ESCRT complexes.', *Critical reviews in biochemistry and molecular biology*. NIH Public Access, 45(6), pp. 463–87. doi: 10.3109/10409238.2010.502516.

Ilieva, H., Polymenidou, M. and Cleveland, D. W. (2009) 'Non-cell autonomous toxicity in neurodegenerative disorders: ALS and beyond', *Journal of Cell Biology*, 187(6), pp. 761–772. doi: 10.1083/jcb.200908164.

Ince, P. G., Highley, J. R., Kirby, J., Wharton, S. B., Takahashi, H., Strong, M. J. and Shaw, P. J. (2011) 'Molecular pathology and genetic advances in amyotrophic lateral sclerosis: An emerging molecular pathway and the significance of glial pathology', *Acta Neuropathologica*, 122(6), pp. 657–671. doi: 10.1007/s00401-011-0913-0.

Isaacs, a M., Johannsen, P., Holm, I. and Nielsen, J. E. (2011) 'Frontotemporal dementia caused by CHMP2B mutations.', *Current Alzheimer research*, 8, pp. 246–51. doi: 10.2174/1567211212225992050.

Jacob, C. P., Koutsileri, E., Bartl, J., Neuen-Jacob, E., Arzberger, T., Zander, N., Ravid, R., Roggendorf, W., Riederer, P. and Grünblatt, E. (2007) 'Alterations in expression of glutamatergic transporters and receptors in sporadic Alzheimer's disease.', *Journal of Alzheimer's disease : JAD*, 11(1), pp. 97–116. Available at: http://www.ncbi.nlm.nih.gov/pubmed/17361039 (Accessed: 1 March 2018).

Jones, V. C., Atkinson-Dell, R., Verkhratsky, A. and Mohamet, L. (2017) 'Aberrant iPSC-derived human astrocytes in Alzheimer's disease', *Cell Death and Disease*, 8(3), p. e2696. doi: 10.1038/cddis.2017.89.

Krasniak, C. S. and Ahmad, S. T. (2016) 'The role of CHMP2BIntron5 in autophagy and frontotemporal dementia', *Brain Research*, October, pp. 151–157. doi: 10.1016/j.brainres.2016.02.051.

Lin, C.-L. G., Kong, Q., Cuny, G. D. and Glicksman, M. A. (2012) 'Glutamate transporter EAAT2: a new target for the treatment of neurodegenerative diseases.', *Future medicinal chemistry*. NIH Public Access, 4(13), pp. 1689–700. doi: 10.4155/fmc.12.122.

Lobsiger, C. S. and Cleveland, D. W. (2007) 'Glial cells as intrinsic components of non-cell-autonomous neurodegenerative disease', *Nat Neurosci*, 10(11), pp. 1355–1360. doi: 10.1038/nn1988.

Malarkey, E. B. and Parpura, V. (2008) 'Mechanisms of glutamate release from astrocytes', *Neurochemistry International*, pp. 142–154. doi: 10.1016/j.neuint.2007.06.005.

Malarkey, E. B. and Parpura, V. (2011) 'Temporal characteristics of vesicular fusion in astrocytes: examination of synaptobrevin 2-laden vesicles at single vesicle resolution.', *The Journal of physiology*, 589(Pt 17), pp. 4271–4300. doi: 10.1113/jphysiol.2011.210435.

Maragakis, N. J. and Rothstein, J. D. (2006) 'Mechanisms of Disease: astrocytes in neurodegenerative disease', *Nature Clinical Practice Neurology*. Nature Publishing Group, 2(12), pp. 679–689. doi: 10.1038/ncpneuro0355.

Marucci, G., Lammi, C., Buccioni, M., Dal Ben, D., Lambertucci, C., Amantini, C., Santoni, G., Kandhavelu, M., Abbracchio, M. P., Lecca, D., Volpini, R. and Cristalli, G. (2011) 'Comparison and optimization of transient transfection methods at human astrocytoma cell line 1321N1', *Analytical Biochemistry*, 414, pp. 300–302. doi: 10.1016/j.ab.2011.02.028.

Meyer, K., Ferraiuolo, L., Miranda, C. J., Likhite, S., McElroy, S., Renusch, S., Ditsworth, D., Lagier-Tourenne, C., Smith, R. A., Ravits, J., Burghes, A. H., Shaw, P. J., Cleveland, D. W., Kolb, S. J. and Kaspar, B. K. (2014) 'Direct conversion of patient fibroblasts demonstrates non-cell autonomous toxicity of astrocytes to motor neurons in familial and sporadic ALS.', *Proceedings of the National Academy of Sciences of the United States of America*, 111(2), pp. 829–32. doi: 10.1073/pnas.1314085111.

Montana, V., Ni, Y., Sunjara, V., Hua, X. and Parpura, V. (2004) 'Vesicular Glutamate Transporter-Dependent Glutamate Release from Astrocytes', *Journal of Neuroscience*, 24(11), pp. 2633–2642. doi: 10.1523/JNEUROSCI.3770-03.2004.

Nagai, M., Re, D. B., Nagata, T., Chalazonitis, A., Jessell, T. M., Wichterle, H. and Przedborski, S.

(2007) 'Astrocytes expressing ALS-linked mutated SOD1 release factors selectively toxic to motor neurons', *Nature Neuroscience*. NIH Public Access, 10(5), pp. 615–622. doi: 10.1038/nn1876.

Ni, Y. and Parpura, V. (2009) 'Dual regulation of Ca $^{2+}$ -dependent glutamate release from astrocytes: Vesicular glutamate transporters and cytosolic glutamate levels', *Glia*, 57(12), pp. 1296–1305. doi: 10.1002/glia.20849.

Oberheim, N. A., Goldman, S. A. and Nedergaard, M. (2012) 'Heterogeneity of astrocytic form and function.', *Methods in molecular biology (Clifton, N.J.)*. NIH Public Access, 814, pp. 23–45. doi: 10.1007/978-1-61779-452-0_3.

Olabarria, M., Noristani, H. N., Verkhratsky, A. and Rodríguez, J. J. (2010) 'Concomitant astroglial atrophy and astrogliosis in a triple transgenic animal model of Alzheimer's disease', *Glia*, 58(7), pp. 831–838. doi: 10.1002/glia.20967.

Pekny, M. and Pekna, M. (2016) 'Reactive gliosis in the pathogenesis of CNS diseases', *Biochimica et Biophysica Acta - Molecular Basis of Disease*. Elsevier, 1862(3), pp. 483–491. doi: 10.1016/j.bbadis.2015.11.014.

Phatnani, H. and Maniatis, T. (2015) 'Astrocytes in neurodegenerative disease.', *Cold Spring Harbor perspectives in biology*. Cold Spring Harbor Laboratory Press, 7(6). doi: 10.1101/cshperspect.a020628.

Piper, R. C. and Katzmann, D. J. (2007) 'Biogenesis and function of multivesicular bodies.', *Annual review of cell and developmental biology*, 23, pp. 519–47. doi: 10.1146/annurev.cellbio.23.090506.123319.

De Pittà, M. and Brunel, N. (2016) 'Modulation of Synaptic Plasticity by Glutamatergic Gliotransmission: A Modeling Study.', *Neural plasticity*. Hindawi Publishing Corporation, 2016, p. 7607924. doi: 10.1155/2016/7607924.

Radford, R. A., Morsch, M., Rayner, S. L., Cole, N. J., Pountney, D. L. and Chung, R. S. (2015) 'The established and emerging roles of astrocytes and microglia in amyotrophic lateral sclerosis and frontotemporal dementia.', *Frontiers in cellular neuroscience*. Frontiers Media SA, 9(October), p. 414. doi: 10.3389/fncel.2015.00414.

Saheki, Y. and De Camilli, P. (2012) 'Synaptic vesicle endocytosis.', *Cold Spring Harbor perspectives in biology*, 4(9), p. a005645. doi: 10.1101/cshperspect.a005645.

Sandbichler, A. M., Aschberger, T. and Pelster, B. (2013) 'A method to evaluate the efficiency

of transfection reagents in an adherent zebrafish cell line.', *BioResearch open access*. Mary Ann Liebert, Inc., 2(1), pp. 20–7. doi: 10.1089/biores.2012.0287.

Schmidt, O. and Teis, D. (2012) 'The ESCRT machinery', *Current Biology*. Elsevier, 22(4), pp. R116-20. doi: 10.1016/j.cub.2012.01.028.

Schousboe, A. and Waagepetersen, H. S. (2005) 'Role of astrocytes in glutamate homeostasis: implications for excitotoxicity.', *Neurotoxicity research*, 8(3–4), pp. 221–5. Available at: http://www.ncbi.nlm.nih.gov/pubmed/16371316 (Accessed: 30 August 2017).

Stuchell-Brereton, M. D., Skalicky, J. J., Kieffer, C., Karren, M. A., Ghaffarian, S. and Sundquist, W. I. (2007) 'ESCRT-III recognition by VPS4 ATPases.', *Nature*, 449(7163), pp. 740–744. doi: 10.1038/nature06172.

Taylor, S. C., Berkelman, T., Yadav, G. and Hammond, M. (2013) 'A defined methodology for reliable quantification of Western blot data.', *Molecular biotechnology*. Springer, 55(3), pp. 217–26. doi: 10.1007/s12033-013-9672-6.

Ugbode, C., Hu, Y., Whalley, B., Peers, C., Rattray, M. and Dallas, M. L. (2017) 'Astrocytic transporters in Alzheimer's disease', *Biochemical Journal*, 474(3), pp. 333–355. doi: 10.1042/BCJ20160505.

Verkhratsky, A., Parpura, V., Pekna, M., Pekny, M. and Sofroniew, M. (2014) 'Glia in the pathogenesis of neurodegenerative diseases.', *Biochemical Society transactions*. Portland Press Limited, 42(5), pp. 1291–301. doi: 10.1042/BST20140107.

Vernay, A., Therreau, L., Blot, B., Risson, V., Dirrig-Grosch, S., Waegaert, R., Lequeu, T., Sellal, F., Schaeffer, L., Sadoul, R., Loeffler, J.-P. and René, F. (2016) 'A transgenic mouse expressing CHMP2B [intron5] mutant in neurons develops histological and behavioural features of amyotrophic lateral sclerosis and frontotemporal dementia', *Human Molecular Genetics*. Oxford University Press, 25(15), pp. 3341–3360. doi: 10.1093/hmg/ddw182.

Vita, D. J. and Broadie, K. (2017) 'ESCRT-III Membrane Trafficking Misregulation Contributes To Fragile X Syndrome Synaptic Defects', *Scientific Reports*, 7(1), p. 8683. doi: 10.1038/s41598-017-09103-6.

Willén, K., Edgar, J. R., Hasegawa, T., Tanaka, N., Futter, C. E. and Gouras, G. K. (2017) 'Aβ accumulation causes MVB enlargement and is modelled by dominant negative VPS4A', *Molecular Neurodegeneration*, 12(1), p. 61. doi: 10.1186/s13024-017-0203-y.

Woodman, P. (2016) 'ESCRT-III on endosomes: new functions, new activation pathway.', *The*

Biochemical journal. Portland Press Ltd, 473(2), pp. e5-8. doi: 10.1042/BJ20151115.

Yamazaki, Y., Takahashi, T., Hiji, M., Kurashige, T., Izumi, Y., Yamawaki, T. and Matsumoto, M. (2010) 'Immunopositivity for ESCRT-III subunit CHMP2B in granulovacuolar degeneration of neurons in the Alzheimer's disease hippocampus', *Neuroscience Letters*. Elsevier Ireland Ltd, 477(2), pp. 86–90. doi: 10.1016/j.neulet.2010.04.038.

van der Zee, J., Urwin, H., Engelborghs, S., Bruyland, M., Vandenberghe, R., Dermaut, B., De Pooter, T., Peeters, K., Santens, P., De Deyn, P. P., Fisher, E. M., Collinge, J., Isaacs, A. M. and Van Broeckhoven, C. (2008) 'CHMP2B C-truncating mutations in frontotemporal lobar degeneration are associated with an aberrant endosomal phenotype in vitro', *Human Molecular Genetics*, 17(2), pp. 313–322. doi: 10.1093/hmg/ddm309.